ERDC/CHL TR-22-8

US Army Corps
of Engineers®
Engineer Research and
Development Center

ERDC
ENGINEER RESEARCH & DEVELOPMENT CENTER

Low-Sill Control Structure Gate Load Study

Jeremy A. Sharp, Duncan B. Bryant, and Gaurav Savant

May 2022

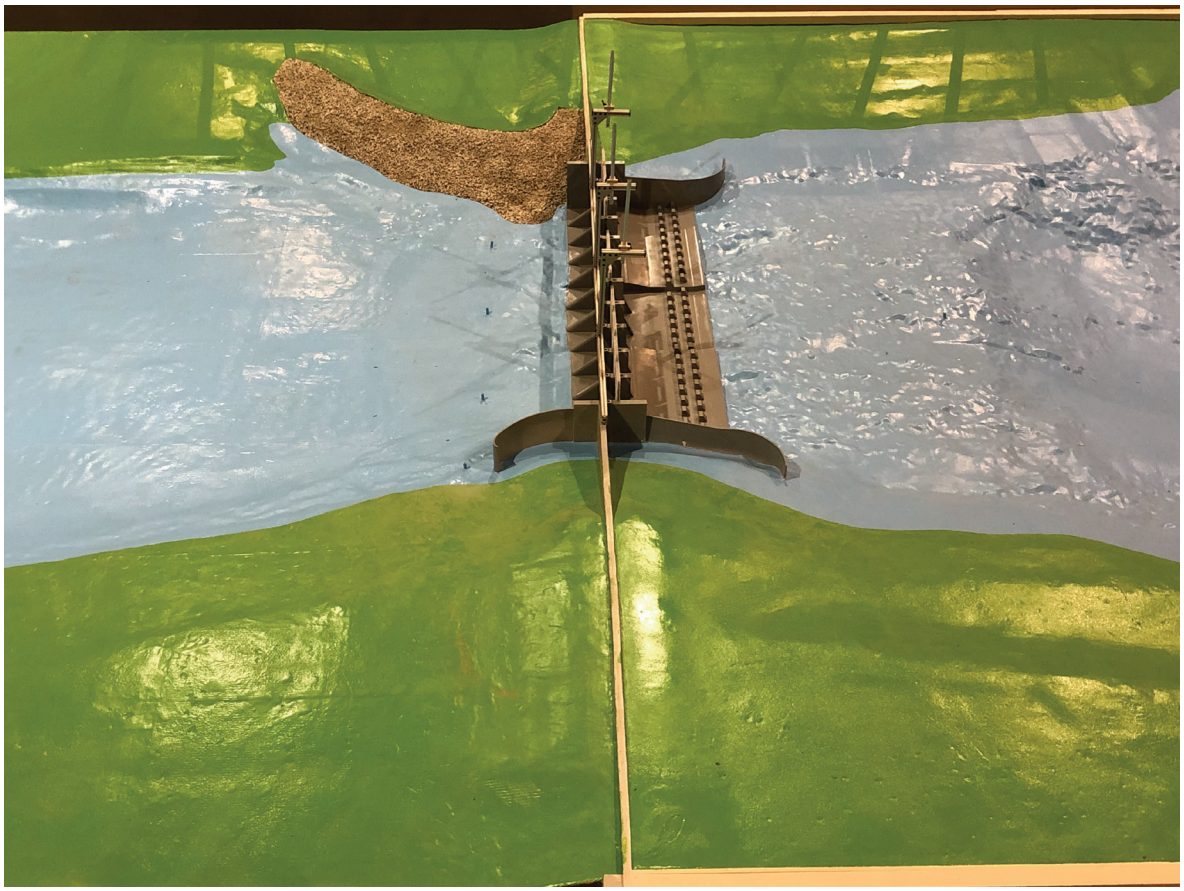

Coastal and Hydraulics Laboratory

The US Army Engineer Research and Development Center (ERDC) solves the nation's toughest engineering and environmental challenges. ERDC develops innovative solutions in civil and military engineering, geospatial sciences, water resources, and environmental sciences for the Army, the Department of Defense, civilian agencies, and our nation's public good. Find out more at www.erdc.usace.army.mil.

To search for other technical reports published by ERDC, visit the ERDC online library at https://erdclibrary.on.worldcat.org/discovery.

ERDC/CHL TR-22-8
May 2022

Low-Sill Control Structure Gate Load Study

Jeremy A. Sharp, Duncan B. Bryant, and Gaurav Savant

Coastal and Hydraulics Laboratory
US Army Engineer Research and Development Center
3909 Halls Ferry Road
Vicksburg, MS 39180-6199

Final report

Prepared for US Army Corps of Engineers, New Orleans District
New Orleans, LA 70118

Under MIPRs W42HEM00279380, W42HEM00772956; "Old River, Low-Sill Control Structure, Physical Model Study"

Abstract

The effort performed here describes the process to determine the gate lifting loads at the Low-Sill Control Structure. To measure the gate loads, a 1:55 Froude-scaled model of the Low-Sill Control Structure was tested. Load cells were placed on 3 of the 11 gates. Tests evaluated the gate loads for various hydraulic heads across the structure. A total of 109 tests were conducted for 14 flows with each flow having two gate settings provided by the United States Army Corps of Engineers, New Orleans District. The load data illustrated the potential for higher gate lifting loads (G_{LL}) to occur at the mid-range gate opening (G_o) for Gates 3 and 6. While for Gate 10, the highest G_{LL} (452 kips, maximum load in testing) was at a G_o = 4.2 ft. Conversely, for the low-flow bays, the highest load occurred at G_o = 24.86 ft.

Contents

Abstract ii

Figures and Tables iv

Preface vi

1 Introduction 1

1.1 Background 2
1.2 Objective 3
1.3 Approach 4

2 Testing Process and Setup 5

2.1 Low-Sill Control Structure (LSCS) Model design 5
2.2 Data collection/instrumentation 8
2.3 Boundary conditions and model operation 10
2.4 Gate lift load calculation 15

3 Results 16

3.1 Water surface elevation (WSE) 16
3.2 Load cell data 25

4 Discussion 37

4.1 Model load 37
4.2 Load impacts from vortex/binding 39
4.3 Flow curvature and super elevation 41

5 Conclusions and Recommendations 43

References 44

Appendix: Adaptive Hydraulics (AdH) Model Development and Application 45

Unit Conversion Factors 53

Acronyms and Abbreviations 54

Report Documentation Page

Figures and Tables

Figures

Figure 1. ORCC location map. 1
Figure 2. Physical model domain configuration as laid over the prototype. 6
Figure 3. Gate bay locations and instrumented bays. 7
Figure 4. Bathymetric contours used in the construction of the LSCS physical model 8
Figure 5. BIF Venturi plot with M3. 9
Figure 6. Load cell rigging. 10
Figure 7. Upstream flow vanes. 12
Figure 8. Flow profiles for Tests 50 and 93. 22
Figure 9. Flow profiles for Tests 6 and 45. 23
Figure 10. Flow profiles for Tests 76 and 38. 24
Figure 11. Gate 3 average and maximum load for set gate openings. 27
Figure 12. Gate 6 average and maximum load for set gate openings. 27
Figure 13. Gate 10 average and maximum load for set gate openings. 28
Figure 14. Flow regime based on headwater, tailwater, and gate opening. Source was digitized from EM 1110-2-1605. 28
Figure 15. Correlation between submerged controlled regime and free controlled regime. 29
Figure 16. Submerged controlled LSCS coefficient vs the measured Q through the structure. 29
Figure 17. Load data from current model study and 1977 model study. 39
Figure 18. Vortex on left side of Gate 3. 40
Figure 19. Types of vortices as defined by the Hydraulic Institute. (Image from Knauss [1987]) 41
Figure 20. Slope of WSE between instrumented gates. 42
Figure 21. Physical model bounding box (flow splits were provided at the upstream locations) 45
Figure 22. Model extents. 46
Figure 23. AdH material types. 47
Figure 24. Rating curve for Baton Rouge. 50
Figure 25. Numerical vs. observed headwaters at LSCS. 51
Figure 26. Example of flow to the LSCS. 52

Tables

Table 1. Physical model scale conversions. 5
Table 2. ORCC flows and WSE for LSCS. 12

Table 3. Gate operation for the LSCS. 13
Table 4. Flow for the LSCS model based on numerical model results. 14
Table 5. Directional fixed vanes angles for Q_M flow. 14
Table 6. Gate properties for model and prototype. 15
Table 7. WSE for all tests. 17
Table 8. Lifting load data from all tests for the three gates tested. 26
Table 9. Gate 3 load data. 30
Table 10. Gate 6 load data. 32
Table 11. Gate 10 load data 35
Table 12. Gate 3 load comparison for prototype and model tests. 37
Table 13. Gate 6 load comparison for prototype and model tests 38
Table 14. Test conditions from current model study and 1977 model study. 38
Table 15. Roughness parameters. 48
Table 16. Flow and headwater scenarios simulated. 49

Preface

This study was conducted for the US Army Engineer District, New Orleans (MVN), under project identification "Old River, Low-Sill Control Structure, Physical Model Study," MIPRs W42HEM00279380, W42HEM00772956. The technical monitor for the MVN was Mr. David Ramirez, Hydraulics and Hydrology branch chief.

The work was performed by the River and Estuarine Engineering Branch of the Flood and Storm Protection Division, US Army Engineer Research and Development Center, Coastal and Hydraulics Laboratory (ERDC-CHL). At the time of publication of this report, Mr. David P. May was branch chief; Dr. Cary A. Talbot was division chief; and Dr. Julie D. Rosati was the technical director for the Flood and Coastal Risk Management Research and Development. The deputy director of ERDC-CHL was Mr. Keith Flowers, and the director was Dr. Ty V. Wamsley.

The commander of ERDC was COL Teresa A. Schlosser, and the director was Dr. David W. Pittman.

1 Introduction

This US Army Engineer Research and Development Center (ERDC), Coastal and Hydraulics Laboratory (CHL), effort describes the process to determine the gate lifting loads at the Low-Sill Control Structure. The Low-Sill Control Structure (LSCS) is one of four structures that are a part of the Old River Control Complex (ORCC) (Figure 1). The ORCC is located along the west bank of the Mississippi River between river miles 317 and 311. It is approximately 50 mi[1] northwest of Baton Rouge, Louisiana, and approximately 35 mi southwest of Natchez, Mississippi.

Figure 1. ORCC location map.

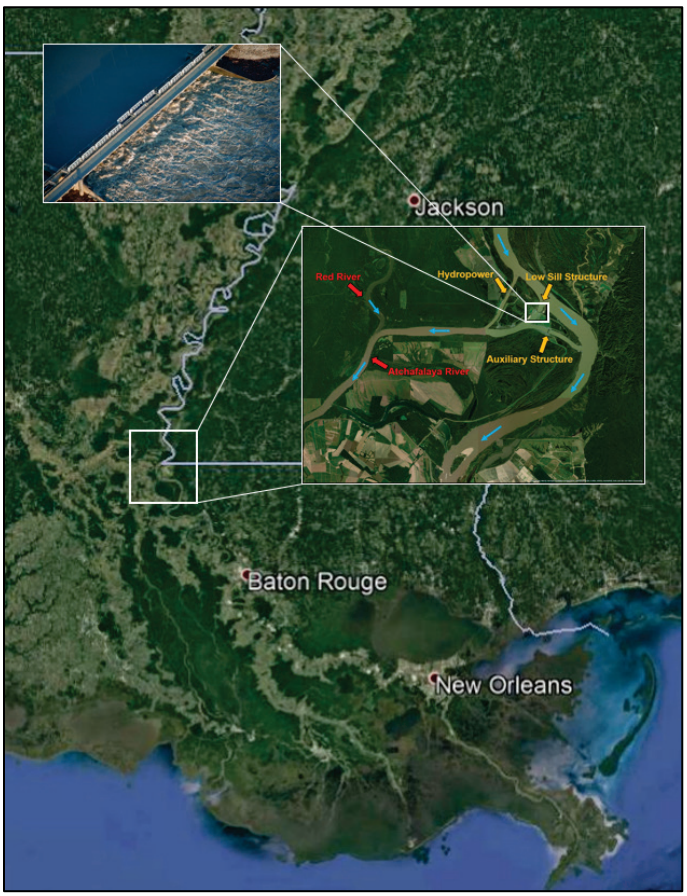

[1] For a full list of the spelled-out forms of the units of measure used in this document, please refer to *US Government Publishing Office Style Manual*, 31st ed. (Washington, DC: US Government Publishing Office 2016), 248-52, https://www.govinfo.gov/content/pkg/GPO-STYLEMANUAL-2016/pdf/GPO-STYLEMANUAL-2016.pdf.

1.1 Background

The ORCC consists of the Sidney A. Murray Hydroelectric Station, the Overbank Structure, the LSCS, and the Auxiliary Structure. Built in the mid-1960s, the LSCS and Overbank Structure were a direct response to concern about losing the Mississippi River down the Atchafalaya River. Since the fifteenth century, there has been a communication between the two systems. The cross-basin flow was exacerbated in the 1830s with the clearing of a natural 40 mi long logjam for navigation and a cutoff that was made near ORCC. In the 1950s, there was an estimated 70/30 percent split between the Mississippi and Atchafalaya Rivers. By law, the ORCC is intended to maintain this split as part of the Mississippi River and Tributaries (MR&T) projects.

A partial failure at LSCS occurred during the flood of 1973, the first high water event experienced by the system since completion of construction. During the event, undermining of the left approach abutment wall occurred causing it to collapse into the entrance channel. Additionally, on the left descending side, a scour hole formed downstream of the structure. As a result of this 1973 event, there was concern of potential flanking or seepage under the LSCS. With the likely possibility of losing the LSCS and thereby the Mississippi River down the Atchafalaya River, the US Army Corps of Engineers (USACE) went into emergency repair operation. Utilizing a Waterways Experiment Station (WES) 1:36 scale model, USACE determined stone launching locations for scour hole filling as the event was ongoing.

After the 1973 event, operational constraints where placed on the allowable head differential across the structure. The design differential of 35 ft was reduced to 22 ft. This limitation reduces the operational capacity of LSCS, thus challenging the ability to maintain the 70/30 split. Additionally, a second structure, the Auxiliary Structure, completed in the 1980s, was built to support the LSCS. To meet some of these challenges associated with increasing the operational range of the LSCS, ERDC CHL constructed a 1:55 Froude-scaled model.

The LSCS was originally designed to pass 350 kcfs with a maximum head differential of 37 ft (USACE WES 1959). The inclusion of the Overbank Structure increases the total design discharge to 600 kcfs. During the flood of 1973, only LSCS was operated, an estimated 480–550 kcfs (with the potential for it to have been even greater) passing the LSCS. This large

discharge resulted in the abutment wall failure. Exacerbated by a low tailwater from the Atchafalaya River side, the high water event on the Mississippi River side created extreme cross currents in the approach channel and caused the failure of the left approach abutment wall. Thus, the structure is now limited to a maximum head differential of 22 ft. Furthermore, studies (Heath et al. 2015) have shown that the Mississippi River is accreting, and stages associated with previous discharges are rising and predicted to continue that trend. As a result, the operation of the LSCS has approached the 22 ft head differential limit more frequently.

ORCC studies have been ongoing since the 1950s and have utilized several physical models at various scales. Of most importance to this effort, an initial gate lifting load study utilizing a 1:36- and 1:60-, general and section model, respectively, showed several concerning features related to the hydraulic performance of the LSCS. These include the tendency for vortex formation, gate leafs to bounce, and high gate leaf lifting loads (USACE 1956). As originally designed, the vertical-lift gates were made up of three to four gate leafs with the intent of their being individually placed in position. However, this proved problematic with gate bouncing. Several attempts were made to eliminate the issue, and the resolution was the pinning of gate leafs together before lowering into the flow. This fastening of the gate leafs helped significantly reduce the bouncing. It was shown that with two leaf sections pinned together, the maximum lifting load experienced was 370 kips (USACE 1956). Thus, from this 1956 study effort, the crane was sized to lift 400 kips. However, the current gate configuration is all the gate leafs are pinned together forming one monolithic gate. It is unclear to the authors the catalyst of the change and why subsequent studies did not evaluate the lifting loads when all the leafs are pinned.

Prototype measurements, shown later in the report, of the lifting loads took place in December 2018. This effort used the current gate configuration of all leafs being pinned. The head differential was 20.7 ft and the loads on Gates 2–7 where measured.

1.2 Objective

The LSCS Physical Model is one of four efforts conducted by ERDC to determine the stability of LSCS and determine an engineering solution for concerns. Specifically, the physical model is measuring the lifting loads of the LSCS gates under various flow conditions. The other efforts include

numerical hydraulic and structure modeling, vibration instrumentation, and ground penetrating radar.

1.3 Approach

The approach to investigate the lifting loads of the various gates for the range of possible hydraulic head differential experienced in the prototype is the implementation of a scaled physical. Currently, this approach is the only option for testing the wide range of potential head differential.

2 Testing Process and Setup

2.1 Low-Sill Control Structure (LSCS) Physical Model design

The LSCS Physical Model is a Froude-scaled 1:55 undistorted model. The model scale conversions are listed in Table 1. The model reproduces a domain that is 5,060 ft long and 1705 ft wide (Figure 2). The scale provides a fully turbulent flow with no surface tension influences for the selected flows. Additionally, the 1:55 scale is a historic scale used at WES for general hydraulic structure models.

The construction method employed for LSCS Physical Model is the Waterways Lightweight Modeling System and is the second physical model built with this method. In all, the LSCS has 1144 ft wide gates siting in three sections (Figure 3). The outer sections (four gates each) are at sill elevations of 10 (North American Vertical Datum 1988 [NAVD 88]) while the inner section (three center gates) is at a sill elevation of -5 (NAVD 88). Each section had an instrumented gate (Gate 3, Gate 6 and Gate 10) with each instrumented gate being three-dimensional (3D) printed out of polymer. To reinforce the 3D printed gate, a 0.125 in. sheet of plate aluminum was epoxied onto the upstream face of the printed gate. The instrumented gates used Teflon slides and waterproof grease and wax to minimize frictional effects. Gate numbering corresponds to the prototype where Gate 1 is the right-most gate, looking downstream.

Table 1. Physical model scale conversions.

Variable	Froude Similitude Scale
Length	L_r = 55
Velocity	$L_r^{0.5}$ = 7.416
Time	$L_r^{0.5}$ = 7.416
Discharge	$L_r^{2.5}$ = 22,434
Volume	L_r^3 = 166,375
Weight	L_r^3 = 166,375

Figure 2. Physical model domain configuration as laid over the prototype.

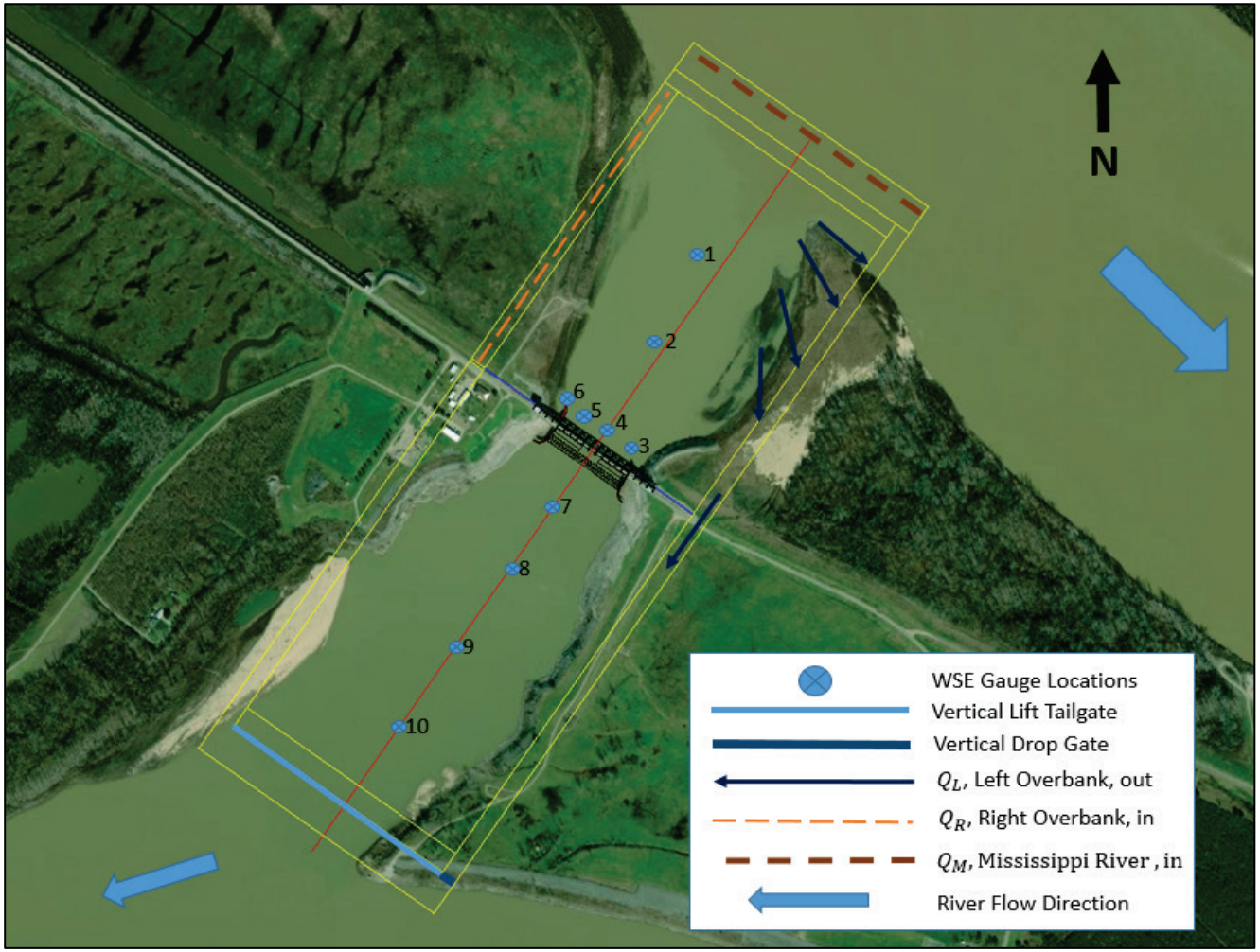

Figure 3. Gate bay locations and instrumented bays.

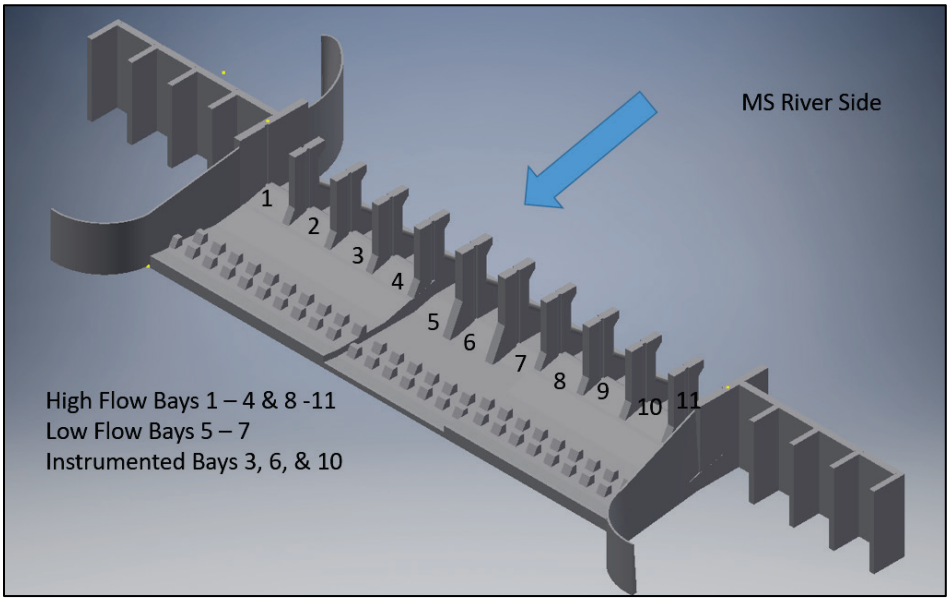

Without using an extremely large domain, which would have been cost prohibitive, the LSCS model design and operation is challenging due to the location of the structure, short approach channel, complexity of overbank flow, and variation in the Mississippi River. To limit the bi-directional flow tendency along the left approach bank to the LSCS, flow operation in the model assumes no overbank operation. Additionally, the hydropower will have a constant outflow of 130 kcfs. Thus, the utilization of a two-dimensional Adaptive Hydraulics (AdH) numerical model provided results for a reasonable domain while allowing for the proper manipulation of flow at the boundary conditions (see the appendix for numerical model details). Figure 4 shows the bathymetry data implemented in the physical model and is from the 2018 survey. The bathymetry is also the same data in the AdH model.

Flow enters into the physical model from two locations: the right overbank flow, Q_R, and the flow entering the mouth of the approach/entrance channel directly from the Mississippi River, Q_M. The Q_M is manipulated by a series of seven flow vans and is varied based on the numerical modeling results. For the Q_L (left overbank flow, out), flow spills over an adjustable sharp-crested weir along the upstream left descending side in the model and is captured in a side channel. The tail water is controlled with a vertical lift gate at the downstream end of the domain.

Note: The horizontal datum is North American Datum 1983 State Plane Louisiana South FIPS 1702 (US feet), and the vertical datum is NAVD 88 (US ft).

Figure 4. Bathymetric contours used in the construction of the LSCS physical model.

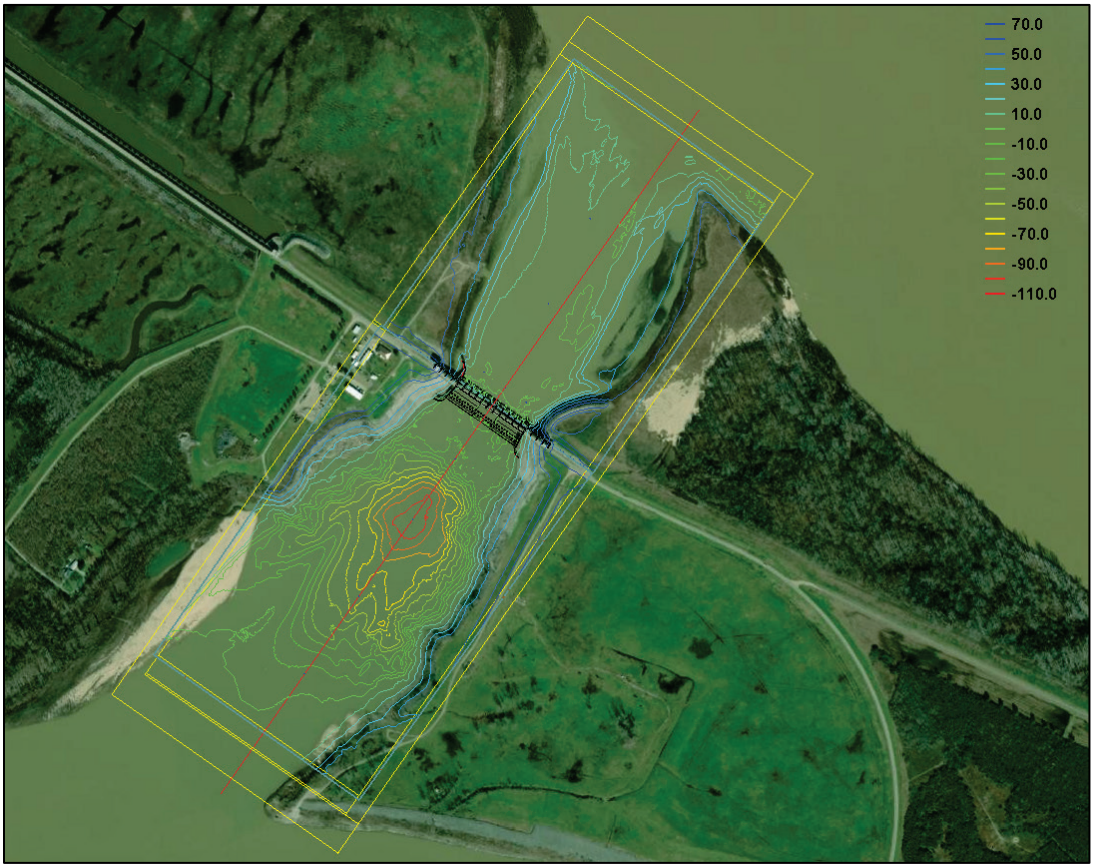

2.2 Data collection/instrumentation

The Q_M measurement utilized a BIF Venturi meter 20 in. Model 0181 Serial Number 97548-1 with manometer using M3 (S.G. = 2.95). Figure 5 shows the plot of head differential and discharge for this Venturi meter. Note the discharge shown in Figure 5 has been converted to prototype. For Q_R discharge measurements, flow was measured using an ultrasonic flowmeter from EESIFLO International. The ultrasonic flow meter accurately measures flow within ± 2% of reading. The left overbank flow Q_L utilized a volumetric measure of flow. Along the left side of the model, there is a 2.02 ft wide, 92 ft long side channel in which overbank flow is captured. At the end of the side channel, there is a vertical drop gate. After the vertical drop gate is rapidly lowered (shut time < 1 sec), the fill rate of the side channel is timed. One foot of depth is equivalent to 186 ft^3.

Figure 5. BIF Venturi plot with M3.

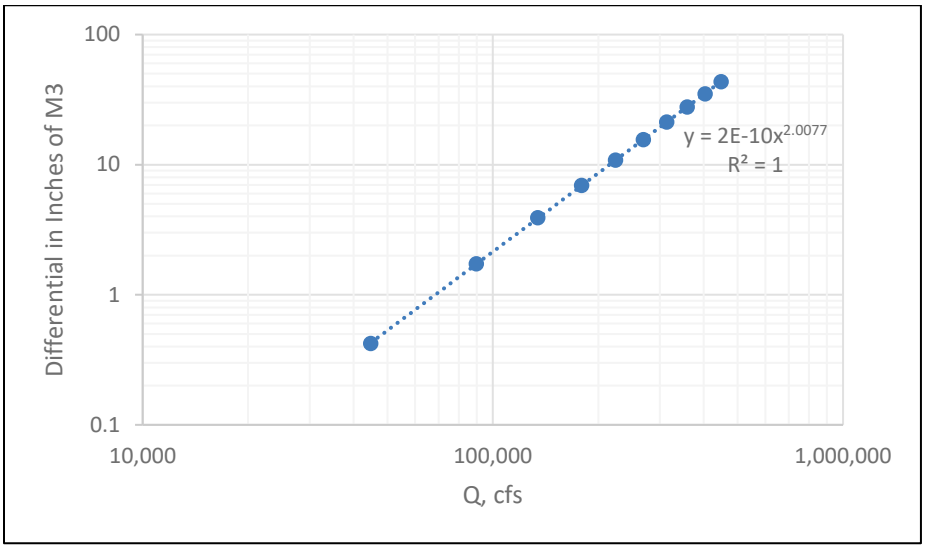

For water surface elevations (WSE) measurements, 10 gauge locations where utilized (Figure 2). These gauge elevations are individually measured with a Leroy Type-A point gauge (error = ± 0.001 ft) in a 5 in. × 5 in. stilling bucket centrally located. Tail water control was established with the mean reading of WSE gauges 7 and 8. The mean between these closely corresponds to River Gage 02100 (longitude: -91.59966600; latitude: 31.07566400). Likewise, for the model headwater control, WSE Gauge 6 is approximately in the same location of River Gage 02050 (longitude: -91.59774400; latitude: 31.07789100). Thus, these model gauges provide the head differential across the structure, ΔH.

The measurement of load on the gates utilized three Futek FSH03941 S-Beam load cells with a maximum tension load capacity of 10 lb. The load cells were attached to an adjustable locking slide to vary gate opening, and each was rigged with braided steel lead lines suspending the load cell between the support slide and gate (Figure 6). The setup prevented the generation of a moment on the load cell. Data collection occurred via a LabView program with a sampling rate of 2000 Hz and a log time of 500 sec. A MatLab code processed the data.

Figure 6. Load cell rigging.

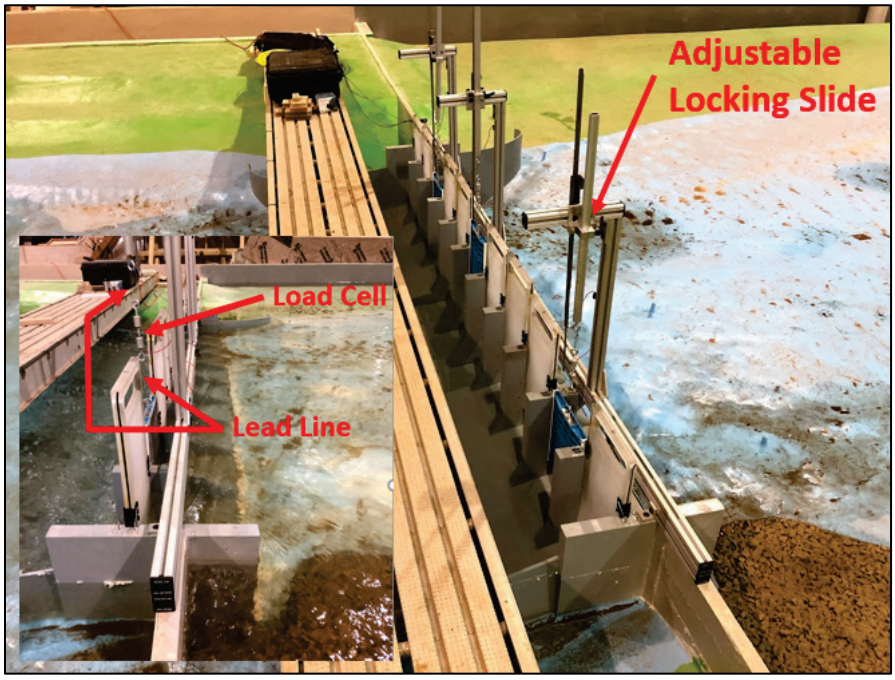

Note: Periodic load cell calibration occurred by using 1, 2, and 5 lb certified weights. The processing code used the calibration curves. The load cells remained within 1%–2% error during the 4-month testing period.

2.3 Boundary conditions and model operation

As previously mentioned, the boundary conditions were established using the results from a numerical model. The numerical modeling work was critical for the proper replication of the flow paths in the model. The primary tools for proper replication of flow paths were a set of flow vanes located at the upstream end of the model (Figure 7), Q_R from a second supply line, and the Q_L overflow weirs. In all, there were 14 flow conditions evaluated (Table 2), and each flow condition had two different gate operations (see Table 3). Note: The percentage flow split shown in Table 2 is Q Simmes/(Q MS + Q Red) for the MR&T 70/30 flow split. Flow splits in the model domain were from the numerical model (Table 4). The flows and gate settings were provided by the New Orleans District (MVN), and each flow condition used the Q_M flow and gate setting 1 or 2 as the test identifier (example: 480 -1, as shown in Table 3).

The directional flow vanes used two key components. First, there was a fixed vane (a total of five) attached to the model's baffle wall via an

adjustable slide, and they also had a slide-out vane section. The sliding vane section allowed for length adjustment to the fixed vane when needed to geometrically fit the alignment. The fixed vane angles came from the flow directions determined using the numerical model and were adjusted for the various flows (Table 5). Vane numbering in the physical model is from 1–5, right to left descending, respectively. The angles were measured clockwise off the baffle wall. Additionally, the fixed vanes where installed on a rail. While these fixed vanes could slide laterally on the rail, via the adjustable slide, this was ultimately not required. The second component were movable vanes that occupied the first 10–12 ft of the upstream end of the model. These movable vanes, as the name implies, were moved as needed to match the flow lines from the AdH model and a total of 6–10 were deployed for the various flows. This was visually verified with dye and review of the AdH numerical model results. While the upstream end of these vanes where typically placed at the downstream end of the fixed vane, model operators would visually adjust the downstream end placement to approximate the flow lines from the numerical models. The development and application of the AdH model used in this study is presented in the appendix.

Testing commenced with the setting of the flow vanes and gate openings. Fixed flow vanes where set with a digital angle finder, error = 0.1°. Gate opening where set with gate gauge blocks (error of 0.005 in.– model or 0.023 ft – prototype). Ultimately, the target tolerance for the fixed vanes is 5°.

Then, using a 20 in. and 8 in. gate valve, the discharges were set. Once the specified Q_M and Q_R were reached, the tailgate was set to meet the tail water control (mean WSE of Gauges 7 and 8). Next, the Q_L was measured via the volumetric method in the side channel. Timing for the volumetric discharge measurement ranged from 40 to 600 sec. There is an estimated error range from 0.19 to 0.01 cfs for this method. The model was considered set for the target conditions when the tail water and head water where within a 0.5 ft tolerance and Q_L was within 10% of the target. To achieve these threshholds, the manipulation of multiple features was required, and it was an iterative process. For first-time flow conditions, it often required multiple days to reach targets/tolerances. Additionally, the Q_L boundary, in the numerical model, had flow lines that would re-enter the model domain, but these where not replicated in the physical model (see the appendix for flow lines from the numerical model).

Figure 7. Upstream flow vanes.

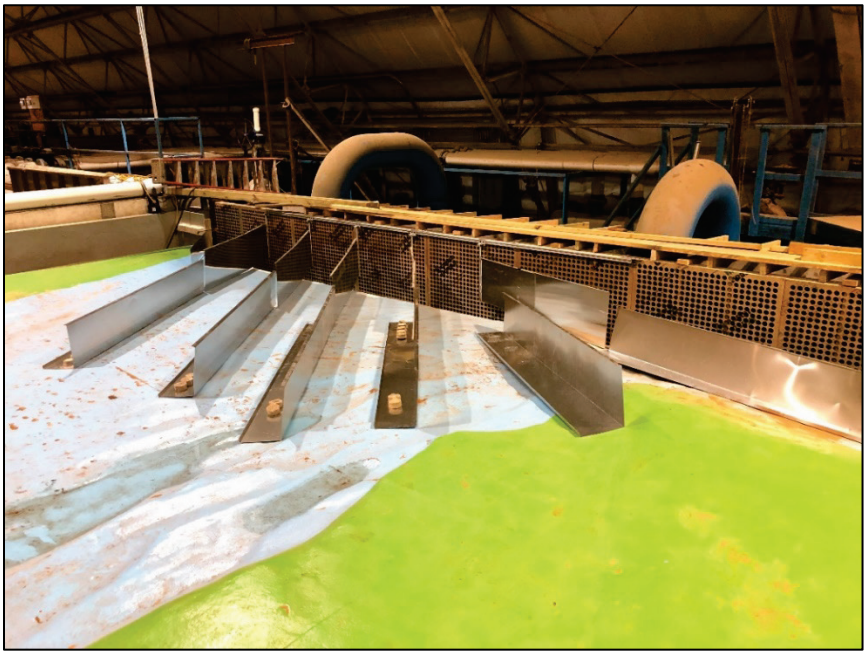

Table 2. ORCC flows and WSE for LSCS.

ORCC and Low Sill Flows and WSE										
LSCS Δ H (ft)	Q MS upstream (kcfs)	HW (ft)	TW (ft)	Q Through Hydropower (kcfs)	Q Through LSCS (kcfs)	Q Simmes (kcfs)	Q RRL (kcfs)	ORCC % Flow Split	RRL Stage (ft)	Q Red (kcfs)
10	480	28	18	130	25	175	325	35	26	20
20	625	36.5	26.5	130	20	275	475	37	34	125
15	640	35	20	130	60	200	450	31	33	10
15	775	40	25	130	70	250	575	30	38	50
20	925	48	28	130	95	300	700	30	46	75
25	1015	52	27	130	85	275	800	26	50	60
30	1100	54	24	130	70	250	900	22	52	50
35	1130	55	20	130	50	200	950	17	52.5	20
15	1480	60	45	130	300	550	1050	34	55	120
10	1530	58	48	130	300	575	1100	34	56	145
20	1550	61	41	130	245	500	1175	30	58.5	125
25	1645	62.5	37.5	130	240	450	1275	26	60	80
30	1650	64	34	130	170	375	1350	22	61.5	75
35	1750	65.5	30.5	130	120	325	1500	18	63	75

Table 3. Gate operation for the LSCS.

Test ID QM - Gate Operation	Gate Openings, feet										
	1	2	3	4	5	6	7	8	9	10	11
480 -1	0.00	4.20	0.00	4.20	4.20	4.20	4.20	4.20	0.00	4.20	0.00
480-2	0.00	0.00	0.00	0.00	11.36	11.36	11.36	0.00	0.00	0.00	0.00
625-1	0.00	4.20	0.00	0.00	4.20	4.20	4.20	0.00	0.00	4.20	0.00
625-2	0.00	0.00	0.00	0.00	7.36	11.36	7.36	0.00	0.00	0.00	0.00
640-1	4.20	4.20	4.20	4.20	7.36	7.36	7.36	4.20	4.20	4.20	4.20
640-2	0.00	0.00	0.00	0.00	19.28	19.28	19.28	0.00	0.00	0.00	0.00
775-1	4.20	7.36	4.20	7.36	7.36	7.36	7.36	7.36	4.20	7.36	4.20
775-2	0.00	0.00	0.00	7.36	19.28	19.28	19.28	7.36	0.00	0.00	0.00
925-1	7.36	7.36	7.36	7.36	7.36	7.36	7.36	7.36	7.36	7.36	7.36
925-2	0.00	0.00	0.00	11.36	19.28	19.28	19.28	11.36	0.00	0.00	0.00
1015-1	4.20	7.36	4.20	4.20	7.36	7.36	7.36	4.20	4.20	7.36	4.20
1015-2	0.00	0.00	0.00	11.36	14.65	14.65	14.65	11.36	0.00	0.00	0.00
1100-1	4.20	4.20	4.20	4.20	4.20	7.36	4.20	4.20	4.20	4.20	4.20
1100-2	0.00	0.00	0.00	7.36	11.36	14.65	11.36	7.36	0.00	0.00	0.00
1130-1	0.00	4.20	0.00	4.20	4.20	4.20	4.20	4.20	0.00	4.20	0.00
1130-2	0.00	0.00	0.00	0.00	11.36	11.36	11.36	0.00	0.00	0.00	0.00
1480-1	24.86	24.86	19.28	24.86	24.86	24.86	24.86	24.86	19.28	24.86	24.86
1480-2	14.65	14.65	19.28	32.69	36.19	36.19	36.19	32.69	19.28	14.65	14.65
1530-1	28.96	28.96	28.96	28.96	32.69	28.96	32.69	28.96	28.96	28.96	28.96
1530-2	19.28	19.28	19.28	36.19	47.15	47.15	47.15	36.19	19.28	19.28	19.28
1550-1	14.65	19.28	14.65	19.28	19.28	19.28	19.28	19.28	14.65	19.28	14.65
1550-2	7.36	11.36	14.65	19.28	32.69	32.69	32.69	19.28	14.65	11.36	7.36
1645-1	14.65	14.65	14.65	14.65	19.28	14.65	19.28	14.65	14.65	14.65	14.65
1645-2	7.36	7.36	14.65	19.28	24.86	24.86	24.86	19.28	14.65	7.36	7.36
1650-1	11.36	11.36	7.36	11.36	11.36	11.36	11.36	11.36	7.36	11.36	11.36
1650-2	0.00	0.00	11.36	14.65	19.28	19.28	19.28	14.65	11.36	0.00	0.00
1750-1	7.36	7.36	4.20	7.36	7.36	7.36	7.36	7.36	4.20	7.36	7.36
1750-2	0.00	0.00	0.00	11.36	19.28	19.28	19.28	11.36	0.00	0.00	0.00

Table 4. Flow for the LSCS model based on numerical model results.

	QT	*QM*	*Δ*M3 *QM*	*QL*	*QR*
Q MS	Total Model Inflow *QT*	*QM* In	Delta, Inches of M3	*QL* Out	*QR* In
480	28,898	28,898	0.18	2,183	NA
625	30,940	30,940	0.20	10,530	NA
640	71,348	71,348	1.09	11,181	NA
775	89,172	89,172	1.70	17,423	NA
925	124,231	124,231	3.31	25,138	NA
1015	122,315	122,315	3.21	37,566	NA
1100	110,427	110,427	2.61	42,660	NA
1130	87,998	87,998	1.66	42,091	NA
1480	357,869	308,630	20.57	66,030	49,239
1530	361,052	306,862	20.33	69,873	54,190
1550	314,212	264,538	15.09	74,068	49,674
1645	318,824	260,056	14.58	83,782	58,768
1650	251,306	200,471	8.65	84,211	50,836
1750	204,954	149,586	4.80	87,114	55,368

Table 5. Directional fixed vanes angles for Q_M flow.

Q MS (kcfs)	Numerical Model ID*				
	AdH - 7	AdH - 6	AdH - 5	AdH - 4	AdH 3
	Physical Model ID (degrees off quadrant IV)				
	1	*2*	*3*	*4*	*5*
480	51	52	43	1	1
625	37	30	27	10	4
640	48	50	42	4	7
775	43	44	38	4	4
925	41	41	41	6	6
1015	35	36	37	21	10
1100	30	37	34	25	11
1130	27	34	29	24	12
1480	46	54	48	31	14
1530	45	53	46	31	14
1550	41	41	42	28	14
1645	39	46	39	27	15
1650	32	39	34	25	15
1750	26	33	27	23	15

*identifier

2.4 Gate lift load calculation

The following equation was applied to calculate the gate lifting loads G_{LL}, or the load the crane would experience.

$$G_{LL} = \{(LC + BF) - G_E\} * {L_R}^3 \quad (1)$$

where

G_{LL} = gate lifting load
LC = load cell
BF = excess buoyancy force (additional volume of model gate)
L_{R^3} = 166,375 (scale factor for weight)
G_E = gate error = (model gate weight–prototype gate weight).

The *LC* value is the measured load from the load cells. Due to material property limitations in the construction of the model gates, the gates are not fully geometrically scaled for all the dimensions. Primarily, the gate member thickness had to be oversized to ensure gate stiffness. Thus, the volume of the model gate is greater than that of the prototype. This results in an additional buoyant force denoted as BF in Equation 1. Additionally, this increase in volume added to the model gate weight and was corrected with G_E in Equation 1. Shown in Table 6 are the model and prototype gate values of weight and volume.

During testing there was a gate failure. The three instrumented gates, which were 3D printed with polymer, yielded due to fatigue from the hydrostatic pressure. The gates where re-flattened, and 0.125 in. aluminum plate was epoxied onto the face of the gates for re-enforcement. The new gate weight and volume were used in tests 26-130 shown in Table 6.

Table 6. Gate properties for model and prototype.

Gate ID	Model				Prototype	
	Tests 1 -25		Tests 26 -130			
	Weight, kips	Volume, ft³	Weight, kips	Volume, ft³	Weight, kips	Volume, ft³
3	252.9	2173.3	484.5	3638.0	239.2	438.184
6	314.4	2806.3	609.8	4656.5	322.4	562.408
10	259.4	2173.3	494.1	3638.0	239.2	438.184

3 Results

Data from 109 tests where collected for the 14 flows and two gate settings provided by MVN. With the exception of three tests, all data are included for the WSE. However, a strenuous evaluation was required for the load data, and multiple tests were removed from the listed data below due to unreliable results or interruptions during the data collection.

3.1 Water surface elevation (WSE)

During testing, all WSE gauge readings were recorded (Table 7). These data points are shown below along with the differential head, ΔH (Equation 2), TW (mean of WSE Gauge 7 and 8), and Q through LSCS as measured in the model. Figure 8–Figure 10 show select WSE profiles in reference to the LSCS section, WSE gauge, and stationing as noted in Rothwell and Grace (1977).

$$\Delta H = HW(WSE_{gauge\,6}) - TW(\overline{WSE_{gauge7\,\&\,8}}) \quad (2)$$

Table 7. WSE for all tests.

Test #	Test ID	Gauge #, Station (gates center is sta 100+00), and WSE										ΔH	TW	Q LSCS
		1	2	3	4	5	6	7	8	9	10			
		85+16	91+78	98+39	98+39	98+39	98+39	104+52	109+67	116+28	122+88			
1	1550-2	61.92	61.65	61.04	60.44	60.99	61.32	38.11	40.91	42.07	42.84	21.8	39.5	262,983
2	1550-2	61.04	60.93	60.55	60.16	60.66	60.99	38.05	40.80	42.18	42.73	21.6	39.4	259,991
3	1550-2	59.78	59.72	59.50	58.73	59.50	59.61	39.87	42.34	43.66	43.72	18.5	41.1	240,976
4	1550-2	61.15	61.21	60.99	60.11	60.93	61.21	39.92	42.34	43.55	44.65	20.1	41.1	250,782
6	1550-2	61.26	61.26	61.04	60.22	61.04	61.15	39.92	42.40	43.50	44.10	20.0	41.2	247,751
7	1550-1	61.15	61.10	60.82	60.60	60.88	61.10	43.17	43.66	44.27	44.32	17.7	43.4	248,820
8	1550-1	62.31	62.20	61.98	61.65	61.87	62.14	42.34	42.78	44.27	44.32	19.6	42.6	247,074
10	1550-1	61.07	60.99	60.77	60.44	60.77	60.88	41.08	42.07	42.67	42.84	19.3	41.6	249,112
11	1550-1	60.88	60.88	60.60	60.33	60.60	60.88	40.86	41.74	42.29	42.45	19.6	41.3	250,584
12	1550-1	61.04	60.93	60.82	60.55	60.77	60.93	40.69	41.79	41.57	42.40	19.7	41.2	252,290
13	1550-1	61.32	61.15	61.04	60.66	60.93	61.15	40.58	41.74	42.29	42.34	20.0	41.2	253,518
14	1650-1	63.24	63.46	63.19	63.13	63.19	63.19	35.63	36.46	36.62	36.57	27.1	36.0	171,291
15	1650-1	63.30	63.57	63.30	63.19	63.30	63.30	36.62	34.81	34.97	34.86	27.6	35.7	184,005
16	1650-1	62.53	62.97	62.64	62.47	62.64	62.64	33.71	34.53	34.75	34.64	28.5	34.1	182,465
17	1650-1	62.75	63.19	62.86	62.75	62.86	62.97	33.65	34.48	34.75	34.70	28.9	34.1	178,031
18	1650-1	63.13	63.46	63.19	63.13	63.19	63.24	33.71	34.53	34.75	34.70	29.1	34.1	180,242
19	1650-1	63.41	63.68	63.52	63.41	63.46	63.63	33.65	34.59	34.81	34.75	29.5	34.1	182,869
20	1650-1	63.96	64.34	64.12	64.01	64.12	64.18	33.82	34.64	34.81	34.81	29.9	34.2	182,400
21	1650-1	64.18	64.51	64.34	64.12	64.40	64.40	33.71	34.64	34.86	34.75	30.2	34.2	187,972
22	1650-2	64.84	65.17	64.95	64.56	64.95	65.00	27.77	31.89	32.50	33.65	35.2	29.8	152,840
23	1650-2	64.40	64.62	64.34	63.96	64.34	64.45	27.55	31.18	32.66	33.76	35.1	29.4	175,809
24	1650-2	64.12	64.34	64.07	63.68	64.01	64.23	27.66	31.23	32.61	33.65	34.8	29.4	171,990
25	1650-2	64.01	64.18	61.21	63.57	63.96	64.07	28.54	33.60	34.37	35.52	33.0	31.1	162,701

Test #	Test ID	Gauge #, Station (gates center is sta 100+00), and WSE										ΔH	TW	Q LSCS
		1	2	3	4	5	6	7	8	9	10			
		85+16	91+78	98+39	98+39	98+39	98+39	104+52	109+67	116+28	122+88			
26	1650-2	64.07	64.34	64.01	63.63	63.96	64.07	29.69	33.21	34.31	35.41	32.6	31.5	164,162
27	1650-2	64.12	64.45	64.07	63.79	64.12	64.23	29.69	33.21	34.37	35.58	32.8	31.5	165,732
28	1750-2	64.67	64.62	64.51	64.18	64.45	64.45	27.88	30.85	32.55	33.49	35.1	29.4	123,015
29	1750-2	64.67	64.89	64.67	64.34	64.51	64.56	30.79	31.29	32.72	33.65	33.5	31.0	124,542
30	1750-2	64.78	64.67	64.51	64.23	64.45	64.51	30.85	31.18	32.50	33.54	33.5	31.0	123,015
31	1750-2	66.43	66.60	66.43	65.61	65.77	65.77	27.44	31.23	32.61	33.65	36.4	29.3	124,651
32	1750-2	65.28	65.39	65.11	64.95	65.11	65.17	27.77	30.74	32.61	33.60	35.9	29.3	123,015
33	1750-2	64.56	64.51	64.34	64.12	64.23	64.34	27.60	31.07	32.61	33.60	35.0	29.3	123,239
34	1750-1	65.44	65.39	65.22	65.22	65.11	65.17	33.10	33.60	33.76	33.76	31.8	33.3	117,688
35	1750-1	65.44	65.44	65.22	65.22	65.17	65.11	30.74	31.29	31.51	31.51	34.1	31.0	122,839
36	1750-1	65.33	65.33	65.11	64.95	65.00	65.00	30.85	31.29	31.51	31.40	33.9	31.1	96,543
37	1750-1	67.70	67.81	67.59	67.59	67.53	67.59	30.96	31.45	31.67	31.62	36.4	31.2	124,427
38	1750-1	67.70	61.61	67.59	67.53	67.48	67.42	30.90	31.45	31.62	31.51	36.2	31.2	122,659
39	1750-1	67.70	67.70	67.53	67.53	67.48	67.48	31.01	31.12	31.29	31.23	36.4	31.1	122,659
40	1645-1	62.58	62.91	62.36	62.25	62.53	62.69	35.96	37.72	38.11	38.27	25.9	36.8	252,442
41	1645-1	63.13	63.46	62.80	62.69	62.97	63.13	36.73	38.44	38.88	38.88	25.5	37.6	252,521
42	1645-1	62.42	62.69	62.20	62.09	62.25	62.42	36.57	38.38	38.71	38.77	24.9	37.5	247,015
43	1645-1	62.42	62.64	62.14	62.09	62.20	62.42	36.73	38.27	38.77	38.71	24.9	37.5	247,015
44	1645-2	62.69	62.86	62.42	61.92	62.47	62.69	36.62	39.10	40.31	40.86	24.8	37.9	230,618
45	1645-2	62.69	63.08	62.75	62.69	62.69	62.80	36.68	38.99	40.53	40.80	25.0	37.8	231,525
46	1645-2	62.42	62.58	62.25	61.76	62.25	62.42	35.96	38.05	39.43	40.03	25.4	37.0	235,592
47	1645-2	63.41	63.57	63.30	62.75	63.19	63.35	37.83	40.20	41.13	41.74	24.3	39.0	226,980
48	1530-1	55.82	56.15	55.82	55.38	55.71	56.37	47.46	48.39	48.89	49.05	8.4	47.9	324,495
49	1530-1	57.63	58.51	58.07	57.58	58.13	58.68	47.90	49.05	49.66	49.71	10.2	48.5	345,309

Test #	Test ID	Gauge #, Station (gates center is sta 100+00), and WSE										ΔH	TW	Q LSCS
		1	2	3	4	5	6	7	8	9	10			
		85+16	91+78	98+39	98+39	98+39	98+39	104+52	109+67	116+28	122+88			
50	1530-1	58.62	59.28	58.90	58.40	58.84	59.45	48.94	49.93	50.59	50.70	10.0	49.4	335,899
51	1530-1	57.08	57.80	57.36	56.75	57.36	58.07	46.91	47.95	48.61	48.83	10.6	47.4	348,396
52	1530-2	57.41	57.58	57.03	55.38	57.25	57.85	43.44	47.02	47.46	48.28	12.6	45.2	347,002
53	1530-2	57.74	58.29	57.80	56.53	57.96	58.40	46.63	49.11	49.60	50.32	10.5	47.9	319,019
55	1530-2	58.24	58.79	58.35	57.14	58.51	58.95	47.18	49.66	50.37	50.98	10.5	48.4	309,737
56	1480-1	59.45	60.00	59.61	59.23	59.61	60.00	44.65	45.59	46.47	46.52	14.9	45.1	304,370
57	1480-1	59.34	60.00	59.61	59.17	59.56	60.05	44.71	46.25	46.58	46.63	14.6	45.5	308,793
58	1480-1	59.39	59.78	59.61	59.12	59.50	60.00	44.65	45.64	46.36	46.47	14.9	45.1	305,855
59	1480-1	60.00	60.55	60.33	59.83	60.16	60.60	45.64	46.52	47.29	47.35	14.5	46.1	297,296
60	1480-1	60.05	60.60	60.38	59.89	60.22	60.60	45.64	46.63	47.35	47.40	14.5	46.1	298,768
61	1480-1	58.07	58.84	58.51	58.02	58.35	58.90	43.11	44.05	45.04	45.15	15.3	43.6	316,190
62	1480-1	58.24	58.62	58.46	58.07	58.40	58.90	43.06	44.16	45.15	45.09	15.3	43.6	316,190
63	1480-2	60.66	60.93	60.71	59.67	60.71	60.99	44.65	46.96	47.62	48.45	15.2	45.8	299,512
64	1480-2	60.22	60.66	60.44	59.34	60.44	60.82	44.21	46.41	47.68	47.73	15.5	45.3	300,290
65	1480-2	60.22	60.93	60.55	59.39	60.49	60.88	44.38	46.96	47.95	48.06	15.2	45.7	300,290
66	1480-2	60.38	60.82	60.44	59.39	60.55	60.93	44.32	46.52	47.51	48.67	15.5	45.4	302,471
67	1480-2	60.05	60.55	60.27	59.23	60.33	60.66	43.88	46.25	47.46	47.73	15.6	45.1	305,337
68	1480-2	59.94	60.55	60.11	59.12	60.16	60.60	44.10	46.30	47.46	47.73	15.4	45.2	304,391
69	1130-1	55.05	54.99	55.05	54.99	54.99	54.99	20.01	20.62	20.84	20.89	34.7	20.3	42,640
70	1130-1	54.94	54.88	54.94	54.83	54.88	54.88	20.07	20.73	20.84	20.95	34.5	20.4	43,210
71	1130-1	54.94	54.94	54.94	54.88	54.88	54.94	20.45	20.89	21.17	21.22	34.3	20.7	43,210
72	1130-1	55.10	55.05	55.16	55.05	55.05	55.05	20.18	20.73	20.95	21.06	34.6	20.5	40,065
73	1130-1	55.10	55.05	55.16	55.05	55.05	55.05	20.18	20.73	20.95	21.06	34.6	20.5	40,065
74	1130-2	55.32	55.27	55.32	55.21	55.27	55.32	20.12	20.34	20.67	20.95	35.1	20.2	50,486

Test #	Test ID	Gauge #, Station (gates center is sta 100+00), and WSE										ΔH	TW	Q LSCS
		1	2	3	4	5	6	7	8	9	10			
		85+16	91+78	98+39	98+39	98+39	98+39	104+52	109+67	116+28	122+88			
75	1130-2	55.32	55.27	55.32	55.21	55.27	55.27	20.07	20.34	20.62	20.89	35.1	20.2	52,755
76	1100-1	54.00	54.00	54.11	54.00	54.06	54.11	23.86	24.30	24.41	24.41	30.0	24.1	66,899
77	1100-1	54.11	54.11	54.17	54.06	54.11	54.11	23.81	24.30	24.41	24.36	30.1	24.1	66,899
78	1100-2	52.79	54.17	54.22	54.11	54.28	54.28	22.82	25.35	26.17	26.83	30.2	24.1	68,632
79	1100-2	52.79	54.22	54.28	54.17	54.33	54.33	22.93	25.35	26.12	26.78	30.2	24.1	68,632
80	1015-1	52.52	52.46	52.57	52.52	52.57	52.57	27.05	27.60	27.77	27.82	25.2	27.3	65,400
81	1015-1	52.46	52.46	52.52	52.46	52.52	52.57	27.00	27.49	27.66	27.71	25.3	27.2	65,400
82	1015-2	52.63	52.57	52.63	52.46	52.74	52.74	26.28	27.99	29.47	29.42	25.6	27.1	93,270
83	1015-2	52.63	52.57	52.63	52.46	52.74	52.74	26.28	27.99	29.47	29.42	25.6	27.1	93,270
84	925-1	48.12	48.28	48.45	48.39	48.45	48.61	27.66	27.99	28.10	28.04	20.8	27.8	103,450
85	925-1	48.17	48.17	48.50	48.50	48.50	48.67	27.49	27.82	27.93	27.88	21.0	27.7	103,450
86	925-2	48.34	48.34	48.56	48.28	48.72	48.72	27.71	29.64	30.52	31.23	20.0	28.7	96,609
87	925-2	48.28	48.34	48.61	48.28	48.67	48.72	27.55	29.64	30.52	31.23	20.1	28.6	96,609
88	775-1	40.58	40.69	40.64	40.64	40.53	40.64	25.13	25.51	25.62	25.68	15.3	25.3	75,237
89	775-1	40.64	40.75	40.69	40.64	40.64	40.75	25.13	25.46	25.62	25.68	15.5	25.3	75,237
90	775-2	40.31	40.36	40.31	40.09	40.14	40.42	24.19	25.84	26.61	27.05	15.4	25.0	73,348
91	775-2	40.31	40.42	40.25	40.09	40.20	40.42	24.14	25.68	26.61	27.11	15.5	24.9	73,348
92	640-1	35.19	35.30	35.19	35.08	35.08	35.14	19.96	20.51	20.62	20.56	14.9	20.2	62,322
93	640-1	35.25	35.30	35.25	35.19	35.14	35.25	20.01	20.51	20.62	20.62	15.0	20.3	62,322
94	640-2	35.52	35.69	35.58	35.30	35.47	35.69	19.02	21.50	22.10	22.38	15.4	20.3	61,352
95	640-2	35.63	35.69	35.63	35.30	35.47	35.74	19.13	21.55	22.16	22.38	15.4	20.3	61,352
96	625-1	36.40	36.40	36.40	36.35	36.40	36.35	25.92	25.90	25.95	25.90	10.4	25.9	18,321
97	625-1	36.51	36.46	36.51	36.51	36.40	36.40	25.84	25.95	25.95	25.90	10.5	25.9	18,321
98	625-2	36.62	36.62	36.62	36.57	36.57	36.51	26.17	26.17	26.17	26.17	10.3	26.2	17,812

Test #	Test ID	Gauge #, Station (gates center is sta 100+00), and WSE										ΔH	TW	Q LSCS
		1	2	3	4	5	6	7	8	9	10			
		85+16	91+78	98+39	98+39	98+39	98+39	104+52	109+67	116+28	122+88			
99	625-2	36.68	36.62	36.62	36.57	36.62	36.62	26.12	26.06	26.12	26.17	10.5	26.1	17,812
100	480-1	28.65	28.59	28.54	28.48	28.48	28.54	17.92	18.14	18.20	18.20	10.5	18.0	21,741
101	480-1	28.70	28.65	28.65	28.59	28.59	28.59	17.92	18.14	18.20	18.20	10.6	18.0	21,741
102	480-2	27.88	27.77	27.82	27.60	27.71	27.93	17.87	18.14	18.25	18.31	9.9	18.0	21,741
103	480-2	27.60	27.55	27.55	27.33	27.49	27.88	17.87	18.14	18.20	18.20	9.9	18.0	21,741
104	1750-2	65.83	65.83	65.55	65.39	65.55	65.66	28.10	31.23	33.10	34.31	36.0	29.7	113,906
105	1750-2	65.77	65.88	65.77	65.44	65.66	65.72	27.88	31.51	33.05	34.26	36.0	29.7	113,906
106	1650-2	64.12	64.12	63.90	63.57	63.90	64.01	32.44	35.52	36.73	37.67	30.0	34.0	154,819
107	1650-2	64.12	64.07	63.90	63.63	63.85	64.01	32.22	35.63	36.62	37.39	30.1	33.9	154,819
108	1650-2	64.12	64.07	63.90	63.63	63.85	64.01	32.22	35.63	36.62	37.39	30.1	33.9	154,819
109	1650-2	64.12	64.07	63.90	63.63	63.85	64.01	32.22	35.63	36.62	37.39	30.1	33.9	154,819

Figure 8. Flow profiles for Tests 50 and 93.

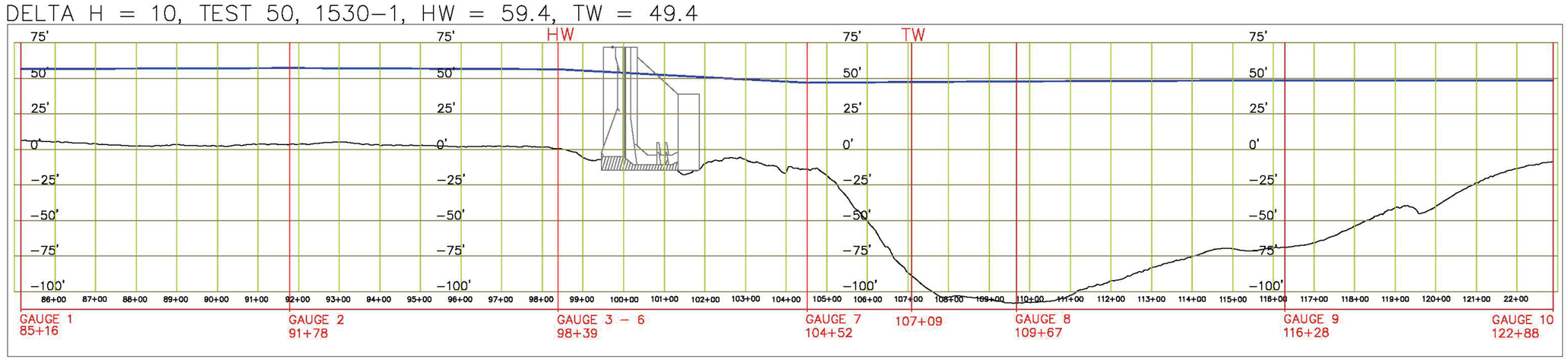

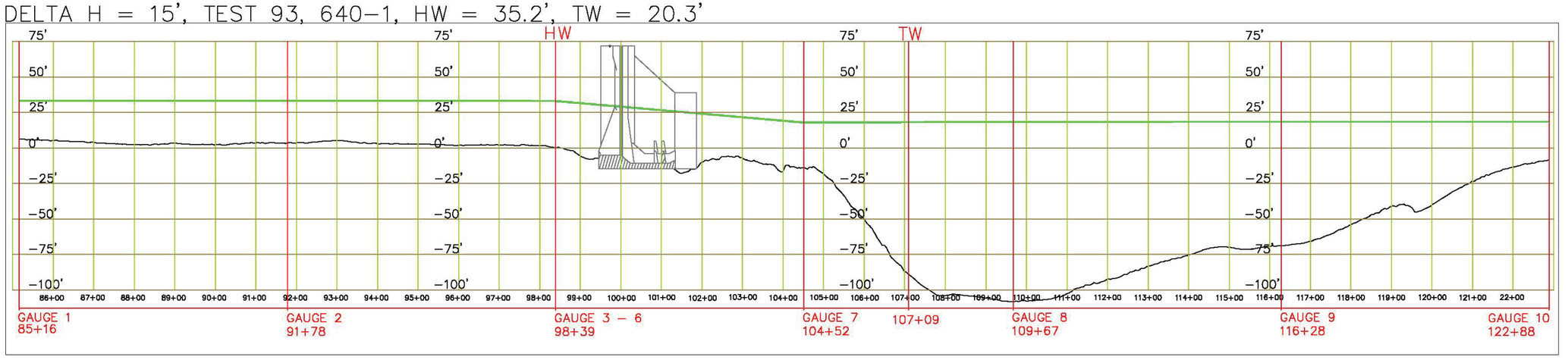

HW = HEADWATER
TW = TAILWATER (MEAN OF GAUGE 7 AND 8)
GATE CENTER = 100+00

Figure 9. Flow profiles for Tests 6 and 45.

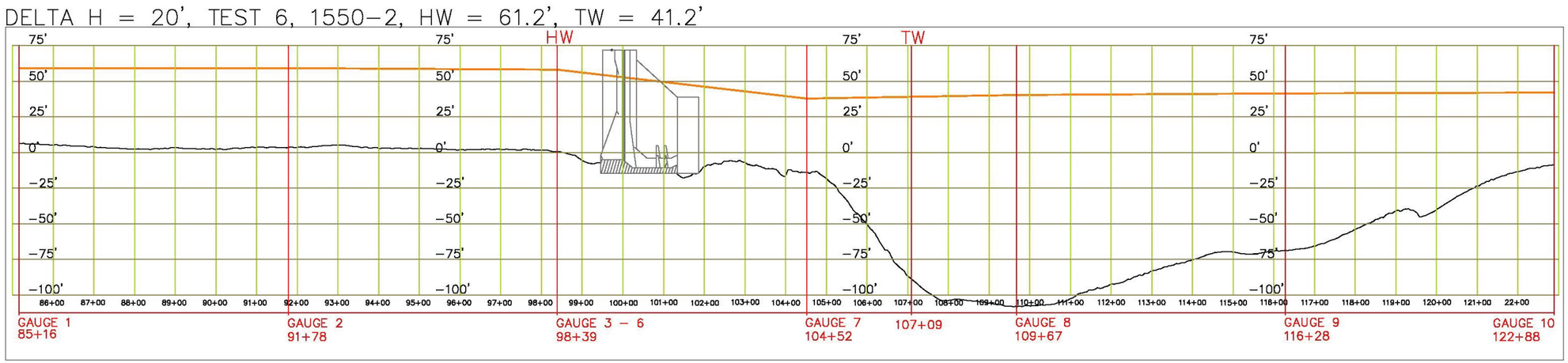

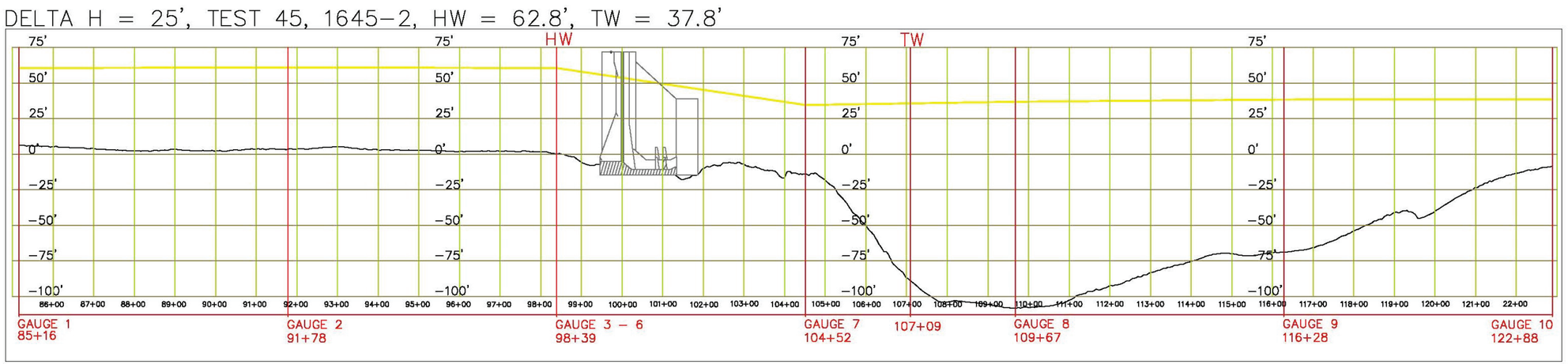

HW = HEADWATER
TW = TAILWATER (MEAN OF GAUGE 7 AND 8)
GATE CENTER = 100+00

Figure 10. Flow profiles for Tests 76 and 38.

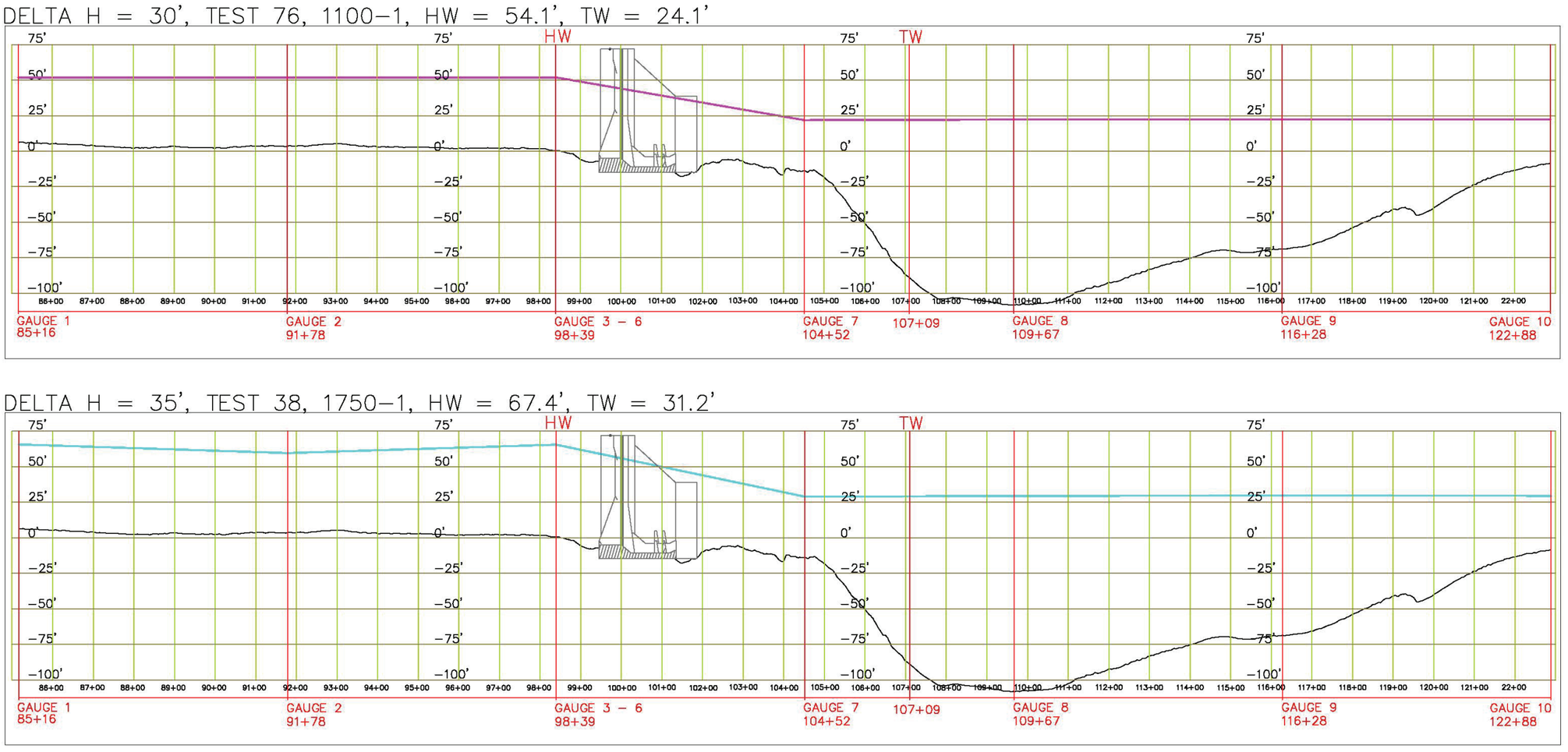

HW = HEADWATER
TW = TAILWATER (MEAN OF GAUGE 7 AND 8)
GATE CENTER = 100+00

3.2 Load cell data

Equation 1 was used to calculate the loads for the tests from the load cell output. The numerical results of these tests are in Table 8. Gate opening, G_o, was used as a sort parameter to subdivide the data (Figure 11–Figure 13). This subdivision of data allowed for the determination of maximum and average lifting loads that the crane experiences for these gate positions. The maximum and average values were averaged over the sample period (5 min @ 2000 Hz); then, the maximum was selected from the specific G_o, and since the sample volume for all the tests is equivalent then for the average, the average of all tests was calculated at the specific G_o (Table 8). Additionally, it allowed for the comparison of the prototype data from the December 2018 gate lift tests. For the two high flow gates, Gates 3 and 10, the maximum load is 344.5 kips and 452.1 kips at an opening of 4.2 ft, respectively (Figure 11 and Figure 13). At the low flow gate, Gate 6, the maximum load is 443.9 kips at an opening of 24.86 ft. The sill elevation for the high flow gates is 10 ft, and for the low flow gates is -5 ft.

The minimum, maximum, and average load data for select tests are in Table 8–Table 11. Additionally, these tables have the following key parameters:

I. G_o
II. ΔH (see Equation 2)
III. h/H (gate submergence, see Equation 3),
IV. Q, SC and Q, FC (calculated gate bay discharge based on the submerged control, SC and free control, FC) see Equation 4 for SC and Equation 5 for FC
V. Percentage of gate submerged (gate submergence divided by gate height).
VI. G (gravity)
VII. 44 is the width of each gate.

Various gate flow regimes require different formulation as shown in EM 1110-2-1605 (USACE 1987). Figure 14 shows the test flows position with respect to their flow regime where the majority are submerged control and free control. The correlation for the two regimes is in Figure 15. Then, the LSCS submerged control coefficient is in Figure 16.

Note: Future use of the LSCS coefficients should be limited to only the gate settings specified in this effort. Extrapolation to other gate settings, not tested, would lead to error resulting in problematic results.

Table 8. Lifting load data from all tests for the three gates tested.

Gate 3		
G_o, ft	AVG of AVG Kips	Max of Max Kips
4.20	232	345
7.36	196	250
11.36	214	240
14.65	228	305
19.28	241	300
28.96	246	266
Gate 6		
4.20	279	349
7.36	259	364
11.36	290	402
14.65	188	415
19.28	296	434
24.86	275	444
28.96	220	323
32.69	283	324
36.19	349	401
47.15	340	357
Gate 10		
4.20	249	452
7.36	222	379
11.36	209	244
14.65	308	433
19.28	235	242
24.86	346	418
28.96	256	287

$$h/H = \frac{TW - Sill\ Elevation}{HW - Sill\ Elevation} \quad (3)$$

$$Q_c = C_{gs} * G_o * 44 * \sqrt{2 * G * \Delta H} \quad (4)$$

$$Q = C_g * 44 * G_o * \sqrt{2 * g * H} \quad (5)$$

Figure 11. Gate 3 average and maximum load for set gate openings.

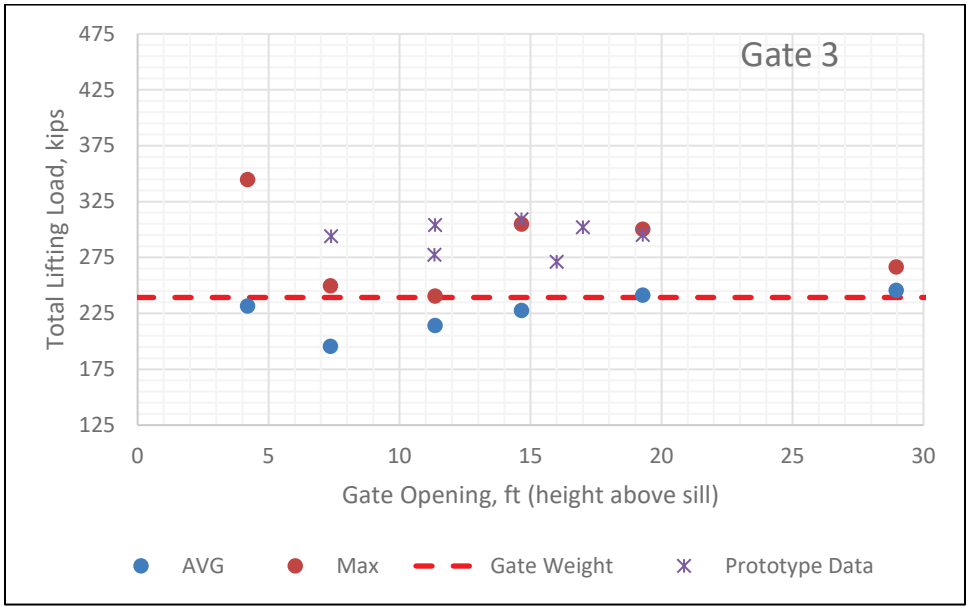

Figure 12. Gate 6 average and maximum load for set gate openings.

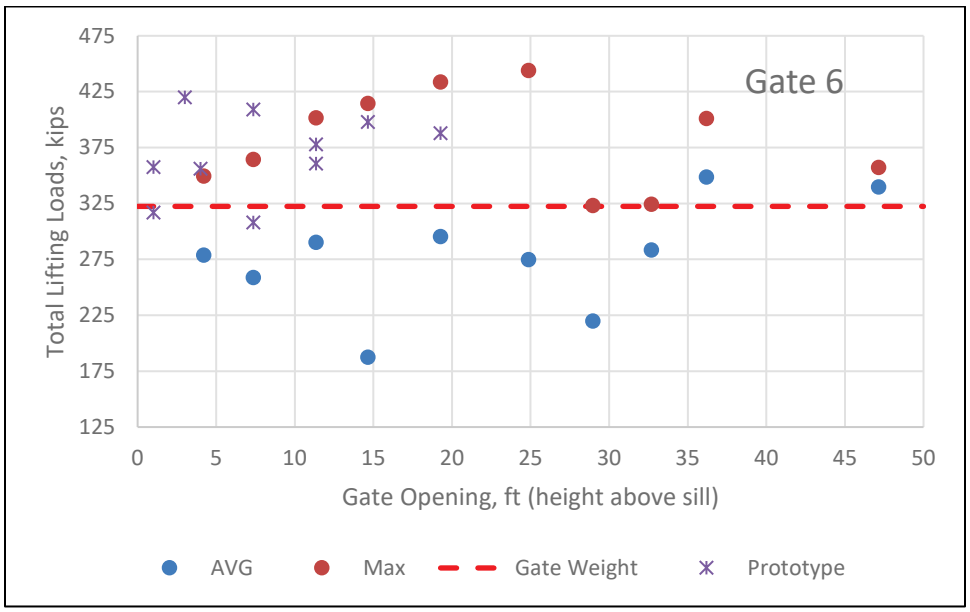

Figure 13. Gate 10 average and maximum load for set gate openings.

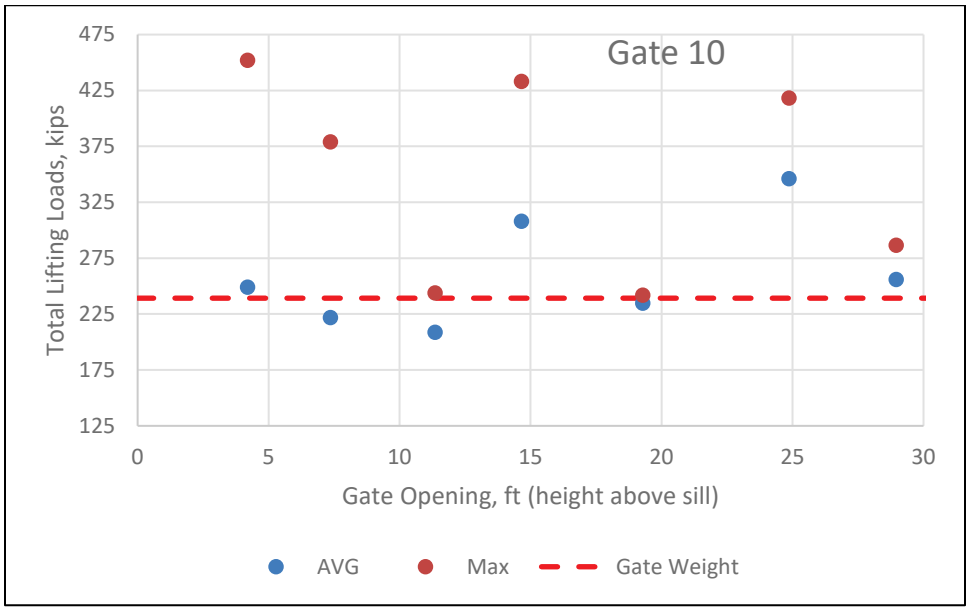

Figure 14. Flow regime based on headwater, tailwater, and gate opening. Source was digitized from EM 1110-2-1605.

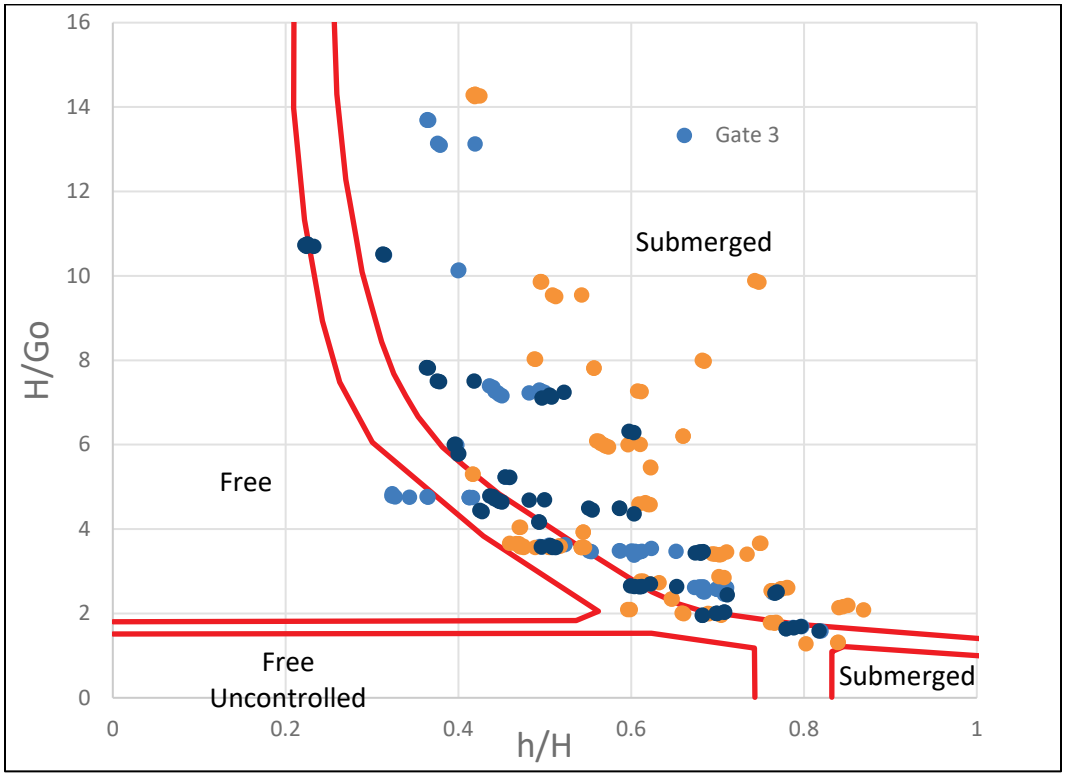

Note: Area between lines represents transition zones fully open gate equivalent to $H/G_o = 0$.

Figure 15. Correlation between submerged controlled regime and free controlled regime.

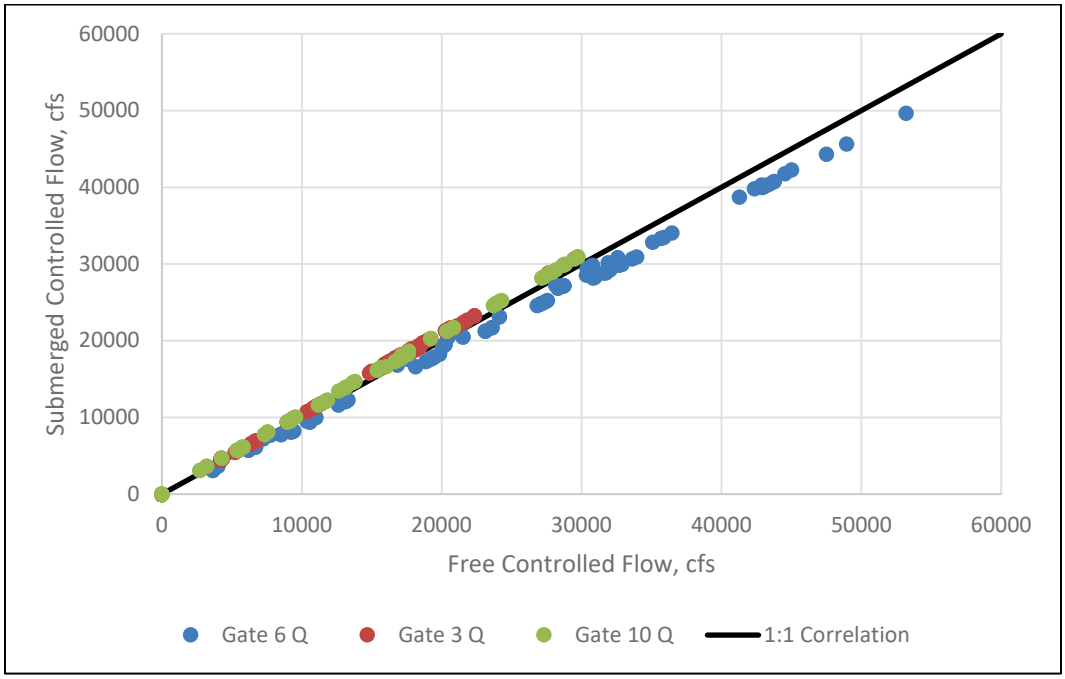

Figure 16. Submerged controlled LSCS coefficient vs the measured Q through the structure.

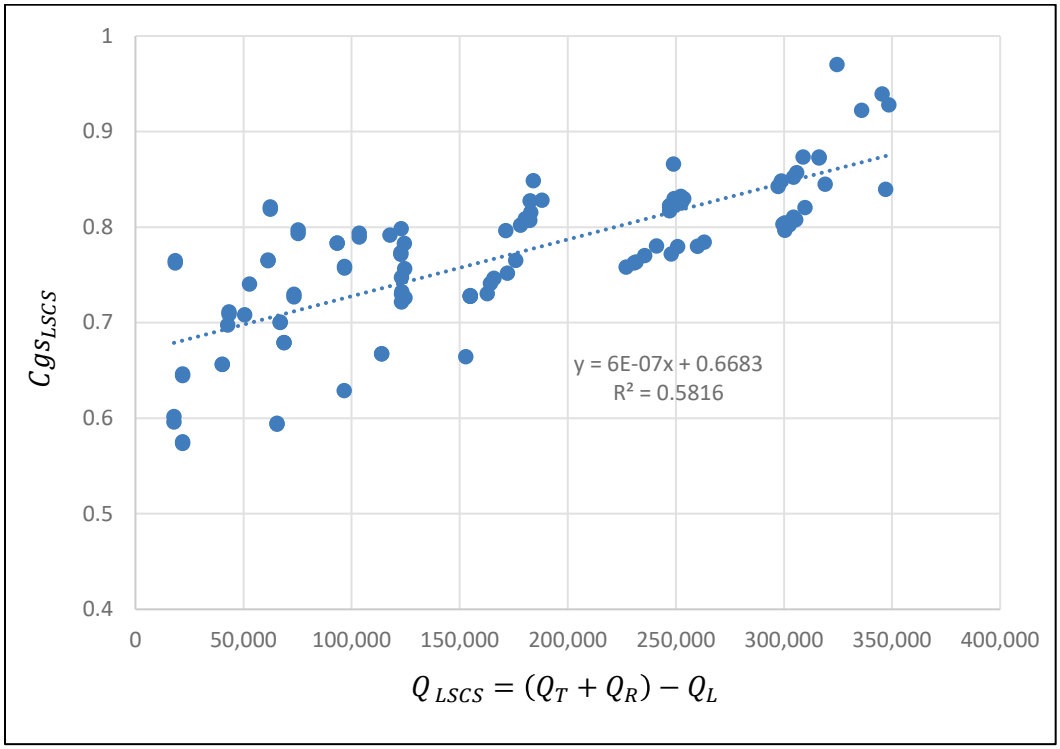

Table 9. Gate 3 load data.

Test #	Test ID	Delta H	*Q* Structure	*Go*	*Q* (FC)	*Q* (SC)	h/H	Average Load	Max	Min	*H/Go*	FC	SC
		ft	CFS	ft	CFS	CFS		Kips	Kips	Kips		Cg	Cgs
36	1750-1	33.9350	96,543	4.20	5233	5432	0.38	234	238	229	13.12	0.58	0.79
37	1750-1	36.3825	124,427	4.20	6754	7002	0.36	227	231	222	13.70	0.60	0.78
38	1750-1	36.2450	122,659	4.20	6657	6902	0.36	210	215	205	13.68	0.59	0.77
39	1750-1	36.4100	122,659	4.20	6658	6902	0.37	211	216	206	13.68	0.59	0.77
76	1100-1	30.0300	66,899	4.20	5419	5692	0.31	138	140	136	10.49	0.55	0.70
80	1015-1	25.2450	65,400	4.20	4188	4430	0.40	139	143	135	10.14	0.43	0.59
88	775-1	15.3175	75,237	4.20	4312	4625	0.50	224	227	221	7.27	0.53	0.80
89	775-1	15.4550	75,237	4.20	4316	4625	0.49	342	345	339	7.29	0.53	0.79
92	640-1	14.9050	62,322	4.20	4253	4701	0.40	273	276	271	5.97	0.57	0.82
93	640-1	14.9875	62,322	4.20	4252	4701	0.40	318	321	315	5.98	0.57	0.82
14	1650-1	27.1425	171,291	7.36	10380	10779	0.48	238	241	237	7.23	0.55	0.80
15	1650-1	27.5825	184,005	7.36	11153	11579	0.50	212	213	210	7.24	0.59	0.85
16	1650-1	28.5175	182,465	7.36	11056	11482	0.45	174	176	172	7.15	0.59	0.83
17	1650-1	28.9025	178,031	7.36	10788	11203	0.45	180	182	179	7.18	0.57	0.80
18	1650-1	29.1225	180,242	7.36	10923	11342	0.45	177	180	175	7.23	0.58	0.81
19	1650-1	29.5075	182,869	7.36	11082	11507	0.44	173	175	170	7.26	0.58	0.82
20	1650-1	29.9475	182,400	7.36	11061	11478	0.44	164	167	161	7.35	0.58	0.81
84	925-1	20.7900	103,450	7.36	8968	9405	0.46	247	250	244	5.22	0.55	0.78
26	1650-2	32.6150	164,162	11.36	15903	16975	0.36	209	214	204	7.39	0.60	0.83
27	1650-2	32.7800	165,732	11.36	16062	17137	0.36	197	202	191	4.76	0.54	0.75
106	1650-2	30.0300	154,819	11.36	14999	16009	0.42	236	240	232	4.74	0.51	0.73
1	1550-2	21.8075	262,983	14.65	17801	18944	0.55	235	236	233	3.48	0.48	0.78
2	1550-2	21.5600	259,991	14.65	17595	18729	0.55	212	216	208	3.46	0.48	0.78
3	1550-2	18.5075	240,976	14.65	16300	17359	0.60	223	225	221	3.38	0.45	0.78
4	1550-2	20.0750	250,782	14.65	16993	18065	0.59	213	215	211	3.48	0.46	0.78
6	1550-2	19.9925	247,751	14.65	16791	17847	0.59	228	230	226	3.48	0.45	0.77
7	1550-1	17.6825	248,820	14.65	18103	18832	0.65	233	234	232	3.47	0.49	0.87
8	1550-1	19.5800	247,074	14.65	17976	18700	0.62	229	230	227	3.54	0.48	0.82
10	1550-1	19.3050	249,112	14.65	18122	18855	0.61	228	229	226	3.47	0.49	0.83
11	1550-1	19.5800	250,584	14.65	18224	18966	0.61	221	223	220	3.45	0.50	0.83

Table 9. Continued.

Test #	Test ID	Delta H	*Q* Structure	*Go*	*Q* (FC)	*Q* (SC)	h/H	Average Load	Max	Min	H/*Go*	FC	SC
		ft	CFS	ft	CFS	CFS		Kips	Kips	Kips		Cg	Cgs
12	1550-1	19.6900	252,290	14.65	18345	19095	0.60	220	221	218	3.47	0.50	0.83
13	1550-1	19.9925	253,518	14.65	18435	19188	0.60	252	254	251	3.48	0.50	0.83
40	1645-1	25.8500	252,442	14.65	20857	21702	0.49	208	215	203	3.59	0.56	0.83
41	1645-1	25.5475	252,521	14.65	20870	21709	0.50	215	220	211	3.62	0.55	0.83
42	1645-1	24.9425	247,015	14.65	20392	21236	0.51	229	233	225	3.57	0.55	0.82
43	1645-1	24.9150	247,015	14.65	20388	21236	0.51	230	235	225	3.56	0.55	0.82
44	1645-2	24.8325	230,618	14.65	18615	19656	0.51	203	207	200	3.58	0.50	0.76
45	1645-2	24.9700	231,525	14.65	18651	19734	0.51	301	305	298	3.60	0.50	0.76
46	1645-2	25.4100	235,592	14.65	19006	20080	0.50	224	228	220	3.57	0.51	0.77
47	1645-2	24.3375	226,980	14.65	18319	19346	0.52	223	227	220	3.63	0.49	0.76
52	1530-2	12.6225	347,002	19.28	19239	20303	0.71	202	205	199	2.45	0.41	0.84
53	1530-2	10.5325	319,019	19.28	17669	18666	0.76	199	203	197	2.49	0.37	0.84
55	1530-2	10.5325	309,737	19.28	17161	18123	0.77	205	209	203	2.52	0.36	0.82
56	1480-1	14.8775	304,370	19.28	21529	22372	0.70	180	183	177	2.57	0.45	0.85
57	1480-1	14.5750	308,793	19.28	21837	22697	0.70	224	228	221	2.57	0.46	0.87
60	1480-1	14.4650	298,768	19.28	21127	21961	0.71	251	256	247	2.60	0.44	0.85
61	1480-1	15.3175	316,190	19.28	22328	23241	0.68	234	239	228	2.51	0.47	0.87
62	1480-1	15.2900	316,190	19.28	22338	23241	0.68	268	272	264	2.51	0.47	0.87
64	1480-2	15.5100	300,290	19.28	20303	21355	0.68	296	300	291	2.62	0.42	0.80
65	1480-2	15.2075	300,290	19.28	20301	21355	0.68	289	293	285	2.62	0.42	0.80
66	1480-2	15.5100	302,471	19.28	20462	21510	0.68	273	279	268	2.62	0.42	0.80
67	1480-2	15.5925	305,337	19.28	20645	21714	0.67	272	276	268	2.61	0.43	0.81
48	1530-1	8.4425	324,495	28.96	27619	28825	0.82	205	208	202	1.58	0.40	0.97
49	1530-1	10.2025	345,309	28.96	29483	30673	0.79	263	266	260	1.66	0.42	0.94
50	1530-1	10.0100	335,899	28.96	28676	29838	0.80	259	262	257	1.69	0.40	0.92
51	1530-1	10.6425	348,396	28.96	29727	30948	0.78	255	258	250	1.64	0.42	0.93

Table 10. Gate 6 load data.

Test #	Test ID	Delta H	*Q* LSCS	*Go*	*Q* (FC)	*Q* (SC)	h/H	Avg Load	Max	Min	H/*Go*	FC	SC
		ft	CFS	ft	CFS	CFS		Kips	Kips	Kips		Cg	Cgs
69	1130-1	34.7	42,640	4.20	6595	6091	0.42	192	294	-63	1.77	0.43	0.81
72	1130-1	34.6	40,065	4.20	6196	5724	0.42	290	294	287	14.24	0.58	0.71
96	625-1	10.4	18,321	4.20	3984	3664	0.75	233	236	230	9.84	0.42	0.76
97	625-1	10.5	18,321	4.20	3986	3664	0.74	347	349	345	9.88	0.42	0.76
100	480-1	10.5	21,741	4.20	3639	3106	0.68	309	313	307	7.97	0.42	0.65
101	480-1	10.6	21,741	4.20	3637	3106	0.68	301	303	299	8.00	0.42	0.64
36	1750-1	33.9	96,543	7.36	10341	9520	0.51	303	310	296	9.54	0.58	0.79
37	1750-1	36.4	124,427	7.36	13295	12269	0.50	297	304	290	9.86	0.60	0.78
38	1750-1	36.2	122,659	7.36	13104	12095	0.49	272	279	266	9.85	0.59	0.77
39	1750-1	36.4	122,659	7.36	13107	12095	0.50	280	288	272	9.85	0.59	0.77
76	1100-1	30.0	66,899	7.36	10990	9975	0.49	88	91	85	8.02	0.55	0.70
84	925-1	20.8	103,450	7.36	10568	9405	0.61	136	139	133	3.92	0.55	0.78
88	775-1	15.3	75,237	7.36	9240	8105	0.66	298	301	294	6.20	0.53	0.80
92	640-1	14.9	62,322	7.36	9421	8238	0.62	295	298	293	5.45	0.57	0.82
93	640-1	15.0	62,322	7.36	9422	8238	0.62	362	364	359	5.46	0.57	0.82
14	1650-1	27.1	171,291	11.36	18134	16637	0.60	267	269	265	6.00	0.55	0.80
15	1650-1	27.6	184,005	11.36	19471	17872	0.61	245	247	243	6.00	0.59	0.85
16	1650-1	28.5	182,465	11.36	19321	17722	0.57	251	253	249	5.94	0.59	0.83
17	1650-1	28.9	178,031	11.36	18851	17292	0.57	259	261	257	5.96	0.57	0.80
18	1650-1	29.1	180,242	11.36	19081	17506	0.57	255	257	253	6.00	0.58	0.81
19	1650-1	29.5	182,869	11.36	19348	17762	0.57	248	250	246	6.02	0.58	0.82
20	1650-1	29.9	182,400	11.36	19279	17716	0.56	234	236	232	6.07	0.58	0.81
74	1130-2	35.1	50,486	11.36	16829	16829	0.42	397	402	392	14.30	0.54	0.66
98	625-2	10.3	17,812	11.36	7759	7759	0.75	291	295	288	3.66	0.30	0.60
99	625-2	10.5	17,812	11.36	7759	7759	0.75	374	377	371	3.66	0.30	0.60
102	480-2	9.9	21,741	11.36	7247	7247	0.70	353	355	351	2.87	0.32	0.57
103	480-2	9.9	21,741	11.36	7247	7247	0.71	312	314	310	2.85	0.32	0.58
40	1645-1	25.9	252,442	14.65	23600	21702	0.61	94	97	90	4.59	0.56	0.83
41	1645-1	25.5	252,521	14.65	23593	21709	0.62	100	103	96	4.62	0.55	0.83
42	1645-1	24.9	247,015	14.65	23106	21236	0.62	96	99	93	4.58	0.55	0.82

Table 10. Continued.

Test #	Test ID	Delta H	*Q* Structure	*Go*	*Q* (FC)	*Q* (SC)	h/H	Average Load	Max	Min	H/*Go*	FC	SC
		ft	CFS	ft	CFS	CFS		Kips	Kips	Kips		Cg	Cgs
43	1645-1	24.9	247,015	14.65	23114	21236	0.62	96	100	93	4.58	0.55	0.82
78	1100-2	30.2	68,632	14.65	20067	19302	0.47	322	327	316	8.02	0.55	0.70
79	1100-2	30.2	68,632	14.65	20066	19302	0.47	410	415	406	4.04	0.50	0.68
82	1015-2	25.6	93,270	14.65	21508	20495	0.54	196	200	190	7.81	0.43	0.59
7	1550-1	17.7	248,820	19.28	27053	24784	0.73	301	303	298	3.40	0.49	0.87
8	1550-1	19.6	247,074	19.28	26817	24610	0.71	293	295	290	3.46	0.48	0.82
10	1550-1	19.3	249,112	19.28	27076	24813	0.70	297	300	295	3.39	0.49	0.83
11	1550-1	19.6	250,584	19.28	27251	24960	0.70	279	282	277	3.39	0.50	0.83
12	1550-1	19.7	252,290	19.28	27432	25130	0.70	274	277	272	3.40	0.50	0.83
13	1550-1	20.0	253,518	19.28	27546	25252	0.69	293	296	291	3.41	0.50	0.83
26	1650-2	32.6	164,162	19.28	30440	28810	0.51	319	324	314	6.08	0.60	0.83
27	1650-2	32.8	165,732	19.28	30733	29085	0.50	304	309	298	3.57	0.54	0.75
28	1750-2	35.1	123,015	19.28	30406	29440	0.48	271	276	266	3.59	0.54	0.73
29	1750-2	33.5	124,542	19.28	30785	29806	0.52	276	284	268	3.60	0.54	0.76
30	1750-2	33.5	123,015	19.28	30409	29440	0.52	274	281	267	3.59	0.54	0.75
31	1750-2	36.4	124,651	19.28	30775	29832	0.46	224	230	219	3.66	0.54	0.73
32	1750-2	35.9	123,015	19.28	30404	29440	0.47	229	234	224	3.63	0.53	0.72
33	1750-2	35.0	123,239	19.28	30472	29494	0.47	236	241	230	3.59	0.54	0.73
86	925-2	20.0	96,609	19.28	24131	23121	0.61	316	319	312	7.27	0.56	0.79
87	925-2	20.1	96,609	19.28	24131	23121	0.61	429	434	424	2.76	0.49	0.76
90	775-2	15.4	73,348	19.28	20233	19489	0.65	328	331	325	2.34	0.44	0.73
91	775-2	15.5	73,348	19.28	20233	19489	0.65	385	388	381	2.34	0.44	0.73
94	640-2	15.4	61,352	19.28	20451	20451	0.60	334	337	330	2.09	0.47	0.76
95	640-2	15.4	61,352	19.28	20451	20451	0.60	339	343	336	2.09	0.47	0.77
104	1750-2	36.0	113,906	19.28	28146	27260	0.47	334	342	327	3.65	0.49	0.67
105	1750-2	36.0	113,906	19.28	28138	27260	0.47	631	645	619	3.65	0.49	0.67
106	1650-2	30.0	154,819	19.28	28712	27170	0.55	168	171	166	3.56	0.51	0.73
44	1645-2	24.8	230,618	24.86	35673	33356	0.62	66	69	62	2.69	0.50	0.76
45	1645-2	25.0	231,525	24.86	35873	33487	0.62	306	312	303	2.72	0.50	0.76
46	1645-2	25.4	235,592	24.86	36454	34075	0.61	312	318	306	2.69	0.51	0.77

Table 10. Continued.

Test #	Test ID	Delta H	*Q* Structure	*Go*	*Q* (FC)	*Q* (SC)	h/H	Average Load	Max	Min	H/*Go*	FC	SC
		ft	CFS	ft	CFS	CFS		Kips	Kips	Kips		Cg	Cgs
47	1645-2	24.3	226,980	24.86	35084	32829	0.63	313	320	307	2.73	0.49	0.76
56	1480-1	14.9	304,370	24.86	31585	28847	0.77	193	195	190	2.58	0.45	0.85
57	1480-1	14.6	308,793	24.86	32041	29266	0.77	294	297	290	2.58	0.46	0.87
60	1480-1	14.5	298,768	24.86	30966	28316	0.78	294	301	289	2.61	0.44	0.85
61	1480-1	15.3	316,190	24.86	32869	29968	0.76	264	268	260	2.53	0.47	0.87
62	1480-1	15.3	316,190	24.86	32879	29968	0.76	433	444	426	2.54	0.47	0.87
48	1530-1	8.4	324,495	28.96	31744	28825	0.87	318	323	313	2.08	0.40	0.97
49	1530-1	10.2	345,309	28.96	33619	30673	0.85	183	187	181	2.16	0.42	0.94
50	1530-1	10.0	335,899	28.96	32671	29838	0.85	191	193	187	2.19	0.40	0.92
51	1530-1	10.6	348,396	28.96	33946	30948	0.84	188	191	185	2.13	0.42	0.93
1	1550-2	21.8	262,983	32.69	45000	42272	0.66	314	316	312	2.00	0.48	0.78
2	1550-2	21.6	259,991	32.69	44530	41791	0.66	282	285	279	1.99	0.48	0.78
3	1550-2	18.5	240,976	32.69	41271	38735	0.70	320	324	316	1.95	0.45	0.78
4	1550-2	20.1	250,782	32.69	42870	40311	0.69	201	203	200	1.99	0.46	0.78
6	1550-2	20.0	247,751	32.69	42353	39824	0.69	299	302	296	1.99	0.45	0.77
63	1480-2	15.2	299,512	36.19	42927	39981	0.77	395	401	390	1.79	0.42	0.80
64	1480-2	15.5	300,290	36.19	43042	40085	0.76	370	375	364	1.78	0.42	0.80
65	1480-2	15.2	300,290	36.19	43033	40085	0.77	364	369	358	1.78	0.42	0.80
66	1480-2	15.5	302,471	36.19	43352	40376	0.77	308	313	304	1.78	0.42	0.80
67	1480-2	15.6	305,337	36.19	43778	40759	0.76	306	310	300	1.77	0.43	0.81
52	1530-2	12.6	347,002	47.15	53187	49653	0.80	353	357	348	1.28	0.41	0.84
53	1530-2	10.5	319,019	47.15	48942	45649	0.84	335	340	330	1.30	0.37	0.84
55	1530-2	10.5	309,737	47.15	47497	44321	0.84	332	337	328	1.32	0.36	0.82

Table 11. Gate 10 load data.

Test #	Test ID	Delta H	*Q* LSCS	*Go*	*Q* (FC)	*Q* (SC)	h/H	Avg Load	Max	Min	H/*Go*	FC	SC
		ft	CFS	ft	CFS	CFS		Kips	Kips	Kips		Cg	Cgs
69	1130-1	34.7	42,640	4.20	5715	6091	0.22	180	213	147	3.42	0.43	0.81
72	1130-1	34.6	40,065	4.20	5373	5724	0.23	219	223	216	10.70	0.58	0.71
76	1100-1	30.0	66,899	4.20	5422	5692	0.31	140	142	138	10.50	0.55	0.70
92	640-1	14.9	62,322	4.20	4262	4701	0.40	198	201	196	6.00	0.57	0.82
93	640-1	15.0	62,322	4.20	4261	4701	0.40	449	452	446	6.01	0.57	0.82
96	625-1	10.4	18,321	4.20	3184	3664	0.60	123	126	121	6.29	0.42	0.76
97	625-1	10.5	18,321	4.20	3185	3664	0.60	329	332	327	6.31	0.42	0.76
100	480-1	10.5	21,741	4.20	2708	3106	0.43	292	294	290	4.41	0.42	0.65
101	480-1	10.6	21,741	4.20	2710	3106	0.42	312	314	310	4.44	0.42	0.64
36	1750-1	33.9	96,543	7.36	9179	9520	0.38	237	241	234	7.50	0.58	0.79
37	1750-1	36.4	124,427	7.36	11841	12269	0.36	231	235	228	7.82	0.60	0.78
38	1750-1	36.2	122,659	7.36	11677	12095	0.36	210	213	206	7.82	0.59	0.77
39	1750-1	36.4	122,659	7.36	11673	12095	0.37	215	218	211	7.82	0.59	0.77
44	1645-2	24.8	230,618	7.36	9347	9875	0.51	18	20	16	7.12	0.50	0.76
45	1645-2	25.0	231,525	7.36	9375	9914	0.51	322	326	320	7.17	0.50	0.76
46	1645-2	25.4	235,592	7.36	9548	10088	0.50	203	206	200	7.10	0.51	0.77
47	1645-2	24.3	226,980	7.36	9213	9719	0.52	207	209	204	7.24	0.49	0.76
80	1015-1	25.2	65,400	7.36	7339	7764	0.40	148	151	144	5.78	0.43	0.59
84	925-1	20.8	103,450	7.36	8968	9405	0.46	259	262	256	5.22	0.55	0.78
88	775-1	15.3	75,237	7.36	7570	8105	0.49	240	242	236	4.16	0.53	0.80
89	775-1	15.5	75,237	7.36	7571	8105	0.49	376	379	373	4.17	0.53	0.79
1	1550-2	21.8	262,983	11.36	13811	14690	0.55	241	243	240	4.49	0.48	0.78
2	1550-2	21.6	259,991	11.36	13629	14523	0.55	209	211	208	4.45	0.48	0.78
3	1550-2	18.5	240,976	11.36	12640	13461	0.60	213	215	211	4.36	0.45	0.78
4	1550-2	20.1	250,782	11.36	13184	14008	0.59	203	205	201	4.49	0.46	0.78
6	1550-2	20.0	247,751	11.36	13021	13839	0.59	212	214	210	4.49	0.45	0.77
14	1650-1	27.1	171,291	11.36	16022	16637	0.48	242	244	240	4.68	0.55	0.80
15	1650-1	27.6	184,005	11.36	17214	17872	0.50	225	227	223	4.69	0.59	0.85
16	1650-1	28.5	182,465	11.36	17065	17722	0.45	193	195	191	4.63	0.59	0.83
17	1650-1	28.9	178,031	11.36	16651	17292	0.45	198	200	196	4.65	0.57	0.80

Table 11. Continued.

Test #	Test ID	Delta H	*Q* Structure	*Go*	*Q* (FC)	*Q* (SC)	h/H	Average Load	Max	Min	H/*Go*	FC	SC
		ft	CFS	ft	CFS	CFS		Kips	Kips	Kips		Cg	Cgs
18	1650-1	29.1	180,242	11.36	16859	17506	0.45	195	197	193	4.68	0.58	0.81
19	1650-1	29.5	182,869	11.36	17113	17762	0.44	191	192	189	4.71	0.58	0.82
20	1650-1	29.9	182,400	11.36	17073	17716	0.44	182	184	181	4.76	0.58	0.81
40	1645-1	25.9	252,442	14.65	20824	21702	0.50	297	302	293	3.57	0.56	0.83
41	1645-1	25.5	252,521	14.65	20837	21709	0.51	302	307	298	3.60	0.55	0.83
42	1645-1	24.9	247,015	14.65	20381	21236	0.51	301	306	297	3.56	0.55	0.82
43	1645-1	24.9	247,015	14.65	20377	21236	0.51	302	306	298	3.56	0.55	0.82
64	1480-2	15.5	300,290	14.65	15427	16227	0.68	426	433	421	3.44	0.42	0.80
65	1480-2	15.2	300,290	14.65	15434	16227	0.68	415	428	404	3.45	0.42	0.80
66	1480-2	15.5	302,471	14.65	15532	16345	0.68	208	212	205	3.44	0.42	0.80
67	1480-2	15.6	305,337	14.65	15679	16500	0.67	213	216	210	3.43	0.43	0.81
7	1550-1	17.7	248,820	19.28	23811	24784	0.65	240	242	239	2.64	0.49	0.87
8	1550-1	19.6	247,074	19.28	23682	24610	0.62	236	238	235	2.70	0.48	0.82
10	1550-1	19.3	249,112	19.28	23849	24813	0.61	233	235	231	2.63	0.49	0.83
11	1550-1	19.6	250,584	19.28	23984	24960	0.61	229	231	227	2.62	0.50	0.83
12	1550-1	19.7	252,290	19.28	24155	25130	0.60	228	230	226	2.64	0.50	0.83
13	1550-1	20.0	253,518	19.28	24288	25252	0.60	237	239	235	2.65	0.50	0.83
52	1530-2	12.6	347,002	19.28	19194	20303	0.71	236	239	232	2.44	0.41	0.84
53	1530-2	10.5	319,019	19.28	17638	18666	0.77	237	240	234	2.48	0.37	0.84
55	1530-2	10.5	309,737	19.28	17132	18123	0.77	237	240	234	2.51	0.36	0.82
56	1480-1	14.9	304,370	24.86	27760	28847	0.70	315	319	312	2.00	0.45	0.85
57	1480-1	14.6	308,793	24.86	28172	29266	0.70	243	245	240	2.00	0.46	0.87
60	1480-1	14.5	298,768	24.86	27286	28316	0.71	393	400	388	2.03	0.44	0.85
61	1480-1	15.3	316,190	24.86	28839	29968	0.68	367	373	361	1.95	0.47	0.87
62	1480-1	15.3	316,190	24.86	28819	29968	0.68	413	418	409	1.95	0.47	0.87
48	1530-1	8.4	324,495	28.96	27652	28825	0.82	180	183	177	1.58	0.40	0.97
49	1530-1	10.2	345,309	28.96	29466	30673	0.79	283	287	280	1.66	0.42	0.94
50	1530-1	10.0	335,899	28.96	28692	29838	0.80	282	285	279	1.69	0.40	0.92
51	1530-1	10.6	348,396	28.96	29727	30948	0.78	278	282	276	1.64	0.42	0.93

4 Discussion

4.1 Model load

The load data illustrated the potential for higher G_{LL} to occur at the mid-range G_o for Gates 3 and 6. While for Gate 10, the highest G_{LL} was at a G_o = 4.2 ft. Conversely, for the low flow bays the highest load occurred at G_o = 24.86 ft. The loads measured in the model typically varied from the loads measured in the prototype, with the exception of gate openings between 10–20 ft. For these openings, there was close agreement using the maximum of the %Δ (Equation 6) with variation of less than 4% and 15% for Gate 3 and 6, respectively (Table 12 and Table 13).

The USACE WES (1956) report indicated the load caused by lifting individual gate leafs instead of pinned gate leaves was un-usable due to large fluctuations in the measurements. The maximum value reported in 1956 was 370 kips.

However, in the Rothwell and Grace (1977) effort, a few vertical load tests were conducted for Gate Bay 6 with three leaves. These load tests were conducted both in a static and opening dynamic conditions. Static refers to measurements obtained with the gate held in a fixed position, and dynamic refers to measurements made while the gate is being raised. Portions of the current model data set compared to this 1977 data set are shown in (Table 14 and Figure 17).

$$\%\Delta = \frac{(Prototype\ G_{LL} - Model\ G_{LL})}{Prototype\ G_{LL}} \quad (6)$$

Table 12. Gate 3 load comparison for prototype and model tests.

Gate 3					
Prototype Test, kips		Model Test, kips		% Δ	
G_o	Load, kips	Average	Maximum	Average	Maximum
7.38	294	195.6	249.5	33.5%	15.1%
11.33	277.3				
11.36	304				
14.65	309	227.6	304.8	26.3%	1.4%
16	271				
17	302				
19.28	295	241.2	300.3	18.2%	-1.8%

Table 13. Gate 6 load comparison for prototype and model tests.

Gate 6							
Prototype Test				Model Test, kips		% Δ	
G_o	Load, kips*	Load, kips**	Avg	Avg	Max	Avg	Max
0	0		0				
1	357.6	317	337.3				
3	420		420				
4***	356		356	278.9	349.5	21.7%	1.8%
7.36	409	308	358.5	259.0	364.5	27.8%	-1.7%
11.36	378	360.6	369.3	290.4	401.6	21.4%	-8.7%
14.65	398		398	187.7	414.6	52.9%	-4.2%
19.28	388		388	295.6	433.6	23.8%	-11.7%

*Load measured when gate was moving up.

**Load measured when gate was moving down.

*** Model G_o was 4.2 ft.

Table 14. Test conditions from current model study and 1977 model study.

Gate 6						
Rothwell and Grace (1977)*						
Test ID	HW, ft	TW, ft	ΔH	Go, ft	GLL, kips	
					Static	Dynamic**
	54.7	46.3	8.4	28.83		368.4
	54.3	47.1	7.2	43.4	356.4	395.4
	51	47	4	47.02	330.4	330.4
Sharp et al. (2022) (data from this current report)						
					Average	Max
52	57.9	45.2	12.6	47.15	352.8	357.2
48	56.4	47.9	8.4	28.96	318.4	323.3

*Two–three gate leaves were used; the fourth one was added to the weight.

**Gates were being moved up.

Figure 17. Load data from current model study and 1977 model study.

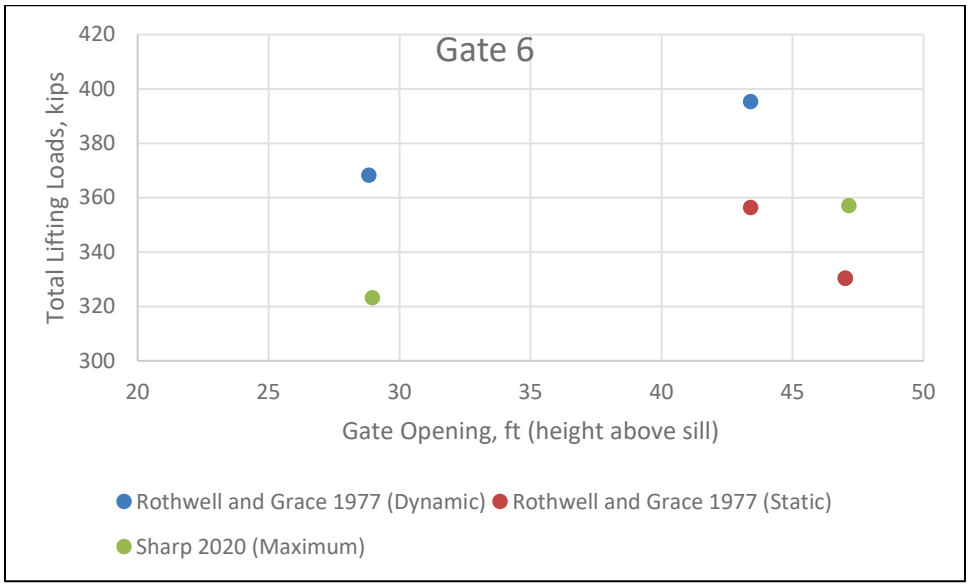

4.2 Load impacts from vortex/binding

Vortices were observed on the upstream side of LSCS in the corner where the pier and gate meet in most of the tests (Figure 18). These vortices are systemic, and even at model scale are considered significant. They have been observed in the prototype, but the authors have found no mention in earlier studies. Often the vortices would occur on both corners and were capable of entraining air and drawing debris, indicative of a Type 4 or 5 vortex on the Alden Research scale of vortex strength (Figure 19). When paper confetti was placed in the flow field, it was quickly drawn under the gates by the vortices. This is a minimum of a Type 4 vortex. Additionally, these air-entraining and debris-capturing vortices would form rollers under the gates, which probably cause fluctuating uplift or downpull loading. By occurring in the corners, asymmetric gate loading is possible. In the model, the gates would get bound by not being level across the bottom of the gate, making it challenging for load cell data interpretation. Often the binding values were identified with repeat tests and would result in either 2–4 times the prior load measurements. When identified, these tests were removed from the load cell data set.

It was also observed that the operator could inadvertently cause a binding on the gates during a gate-setting procedure. This is especially true at some of the higher heads. The research team attempted to countermeasure this issue by allowing for long soak times. These long soak times simply imply the time the gate is set and the appropriate boundary conditions are

met. The soak time was on the order of hours. Any biases that were set accidentally by the operator might work themselves out by allowing the gate to unbind itself via the buoyancy force reaching a stable position. Again, the tests that were believed to have this operator error were also removed from the load cell data set.

As related to the problems at LSCS, it has been well documented in the literature that vortices form an unstable shear layer under flat-bottom gates and excite the elastic gate causing vibration issues on the structure (Thang and Naudascher 1985). This was first shown by Muller (1933).

Figure 18. Vortex on left side of Gate 3.

Figure 19. Types of vortices as defined by the Hydraulic Institute. (Image from Knauss [1987]).

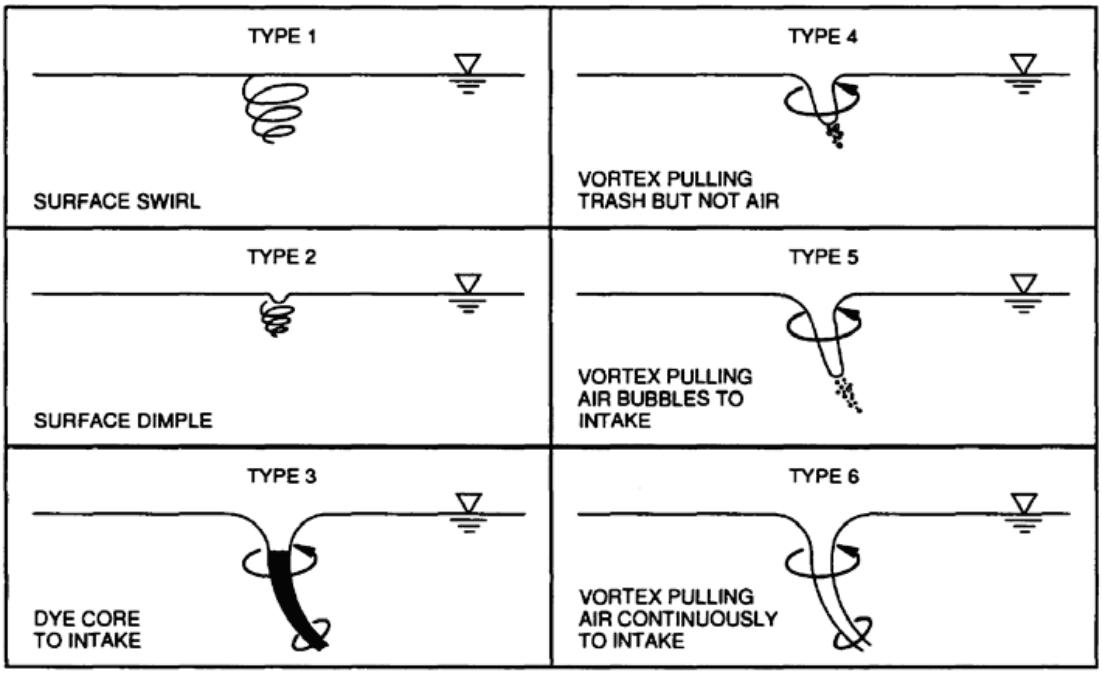

4.3 Flow curvature and super elevation

It was clearly shown in the numerical modeling effort that the approaching flow lines curve into the structure. The curvature into LSCS was originally noted in USACE WES (1956). This flow curvature is naturally occurring due to the geometric location of the LSCS and the Mississippi River. For the flow to enter the structure from the Mississippi River, it must bend, causing a natural setup on the outside. However, for overbank flows, the flow lines are coming across the bank line and exacerbate the issue. Additionally, the entrance channel to the LSCS is hydraulically short with respect to the structures width. With a naturally curving flow, short approach, and overbank flow, there tends to be super-elevation set across the structure. The slope from three instrumented gate bays is shown in Figure 20. As in all cases, the approach flow to the gates should be near uniform allowing for ideal operation and preventing un-needed wear on the structure. At no time was this issue more evident than in the flood of 1973. The flood of 1973 illustrates the potential risk associated with non-uniform approach flow.

Figure 20. Slope of WSE between instrumented gates.

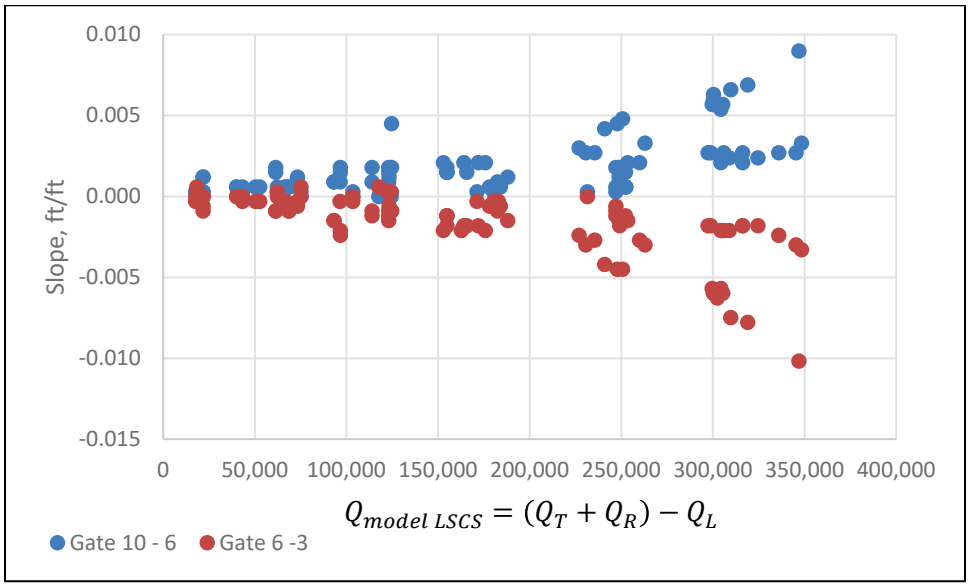

5 Conclusions and Recommendations

- A contributing factor to the severity of the vortex formation is the non-uniform approach flow. The left descending flow is a faster flow thus causing approaching currents to slightly curve into the structure and set up the rotation in the corners. Possible solutions are the following:
  - The installation of bend way weirs to realign the flow as it approaches the structure.
  - Operation of only the Low Flow Bays. This would require the narrowing of the approach channel, and abutment walls would be moved to the bank sides of Gate 5 and 7.
  - Flow-straightening vanes upstream of the structure.
  - Full review of gate operations in the model, such that the gates could limit the frequency or strength of the vortices.
- Of additional concern is the flow separation off the bottom edge of the gates. Poor flow separation can result in vibration, gate bouncing, and gate inefficiencies. To ensure the flow separation from the gate is downstream of the gate and to reduce vibrations, a mitered notch on the bottom edge of the gate could be beneficial. As noted in EM 1110-2-1602 (USACE [1980]), "the 45-deg gate lip should terminate in a 1-in vertical extension to ensure that the jet springs free from the upstream edge of the lip" (page 4–8).
- To further reduce the uncertainty in the model's G_{LL}, tests should be conducted where there is a uniform gate opening for all gates. Then, the ΔH would be maintained at the desired differential. This style of operation would limit some of the uncertainty associated with the multiple G_o.
- Verification testing with the prototype data was started but had to be abandoned due to schedule constraints. It is recommended that this portion of additional testing be conducted.

References

ERDC (US Army Engineer Research and Development Center). 2017. *Adaptive Hydraulics 2D Shallow Water (AdH-SW2D) User Manual* (Version 4.6).

Heath, R. E., G. L. Brown, C. D. Little, T. C. Pratt, J. J. Ratcliff, D. D. Abraham, D. W. Perkey, N. B. Ganesh, K. S. Martin, and D. P. May. 2015. *Old River Control Complex Sedimentation Investigation*. MRG&P Report No. 6. Vicksburg, MS: US Army Engineer Research and Development Center.

Knauss, J. 1987. *Swirling Flow Problems at Intakes*. Hydraulic Structures Design Manual, 1AA. Balkema, Rotterdam.

Muller, O. 1933. Schwingungsuntersuchungen an unterströmten Wehren, Mitt. Preuss. Versuchsanst. f. Wasser- und Schiffbau, Berlin, Vol. 13, 1933. https://scholar.google.com/scholar?hl=en&as_sdt=0%2C25&q=Schwingungsuntersuchungen+an+unterstr%C3%B6mten+Wehren&btnG=

Rothwell, E. D., and J. L. Grace. 1977. *Old River Existing Low-Sill Control Structure, Louisiana: Hydraulic Model Investigation: Final Report*. H-77-2. Vicksburg, MS: US Army Engineer Waterways Experiment Station.

Savant, G., R. C. Berger, G. L. Brown, and C. J. Trahan. 2020. *Theory, Formulation, and Implementation of the Cartesian and Spherical Coordinate Two-Dimensional Depth-Averaged Module of the Adaptive Hydraulics (AdH) Finite Element Numerical Code*. ERDC TR-20-8. Vicksburg, MS: US Army Engineer Research and Development Center.

Thang, N. D., and E. Naudascher. 1986. "Vortex-Excited Vibrations of Underflow Gates." *Journal of Hydraulic Research* 24(2): 133–151.

USACE. 1980. *Hydraulic Design of Reservior Outlet Works*. EM 1110-2-1602. Washington, DC: US Army Corps of Engineers.

USACE. 1987. *Hydraulic Design of Navigation Dams*. EM 1110-2-1605. Washington, DC: US Army Corps of Engineers.

USACE WES (US Army Corps of Engineers, Waterways Experiment Station). 1956. *Old River Low-Sill Control Structure, Downpull Force on Vertical-Lift Gates*. Technical Report No. 2-447, Report 1. Vicksburg, MS: US Army Engineer Waterways Experiment Station.

USACE WES. 1959. *Old River Low-Sill Control Structure, Study of Overall Performance*. Technical Report No. 2-447, Report 3. Vicksburg, MS: US Army Engineer, Waterways Experiment Station.

Appendix: Adaptive Hydraulics (AdH) Model Development and Application

The main objective of the AdH numerical modeling effort was to provide the flow splits including flow angles to the physical model of the Low Sill Structure being developed at the ERDC (Figure 21). The model domain extended from Natchez, MS, to Baton Rouge, LA (Figure 22). The model vertical datum was the NAVD88, and the horizontal datum was State Plane: Louisiana South (meters).

Figure 21. Physical model bounding box (flow splits were provided at the upstream locations).

The AdH model was executed in the International System of Units (SI), and the results were converted to English units for presentation here.

Figure 22. Model extents.

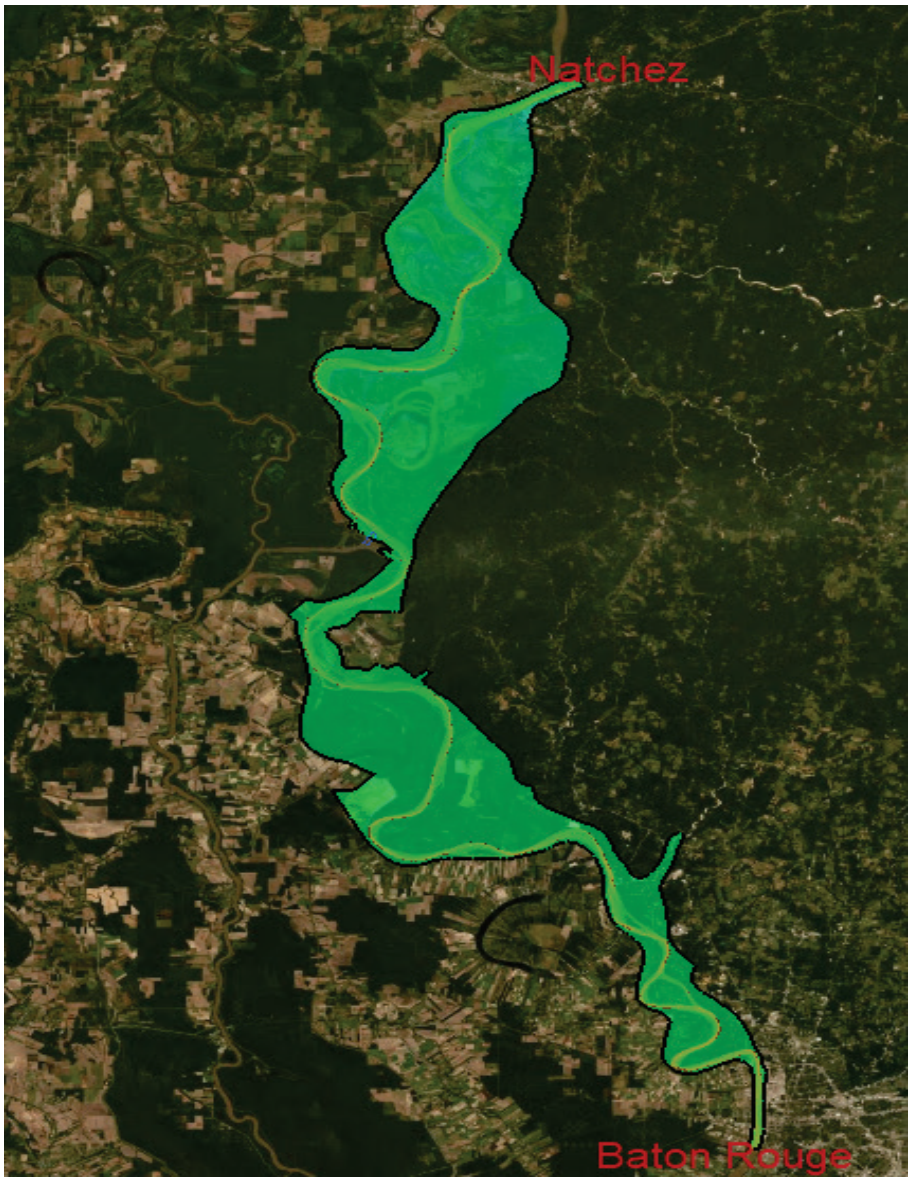

AdH allows the user to specify roughness using physical parameters such as vegetation density, vegetation diameters in addition to Manning's roughness (Savant et al. 2020). Since the aim of this numerical model application was to provide flow information to the physical model over a wide range of flows including flows that inundate the floodplain, the ability to represent losses due to vegetation was utilized. Further information for the AdH code is in ERDC 2017. To adequately represent the variable land use within the model extents, the domain was discretized using variable bottom stress, friction, and flow regime. A description of these is provided in Figure 23 and Table 15.

Figure 23. AdH material types.

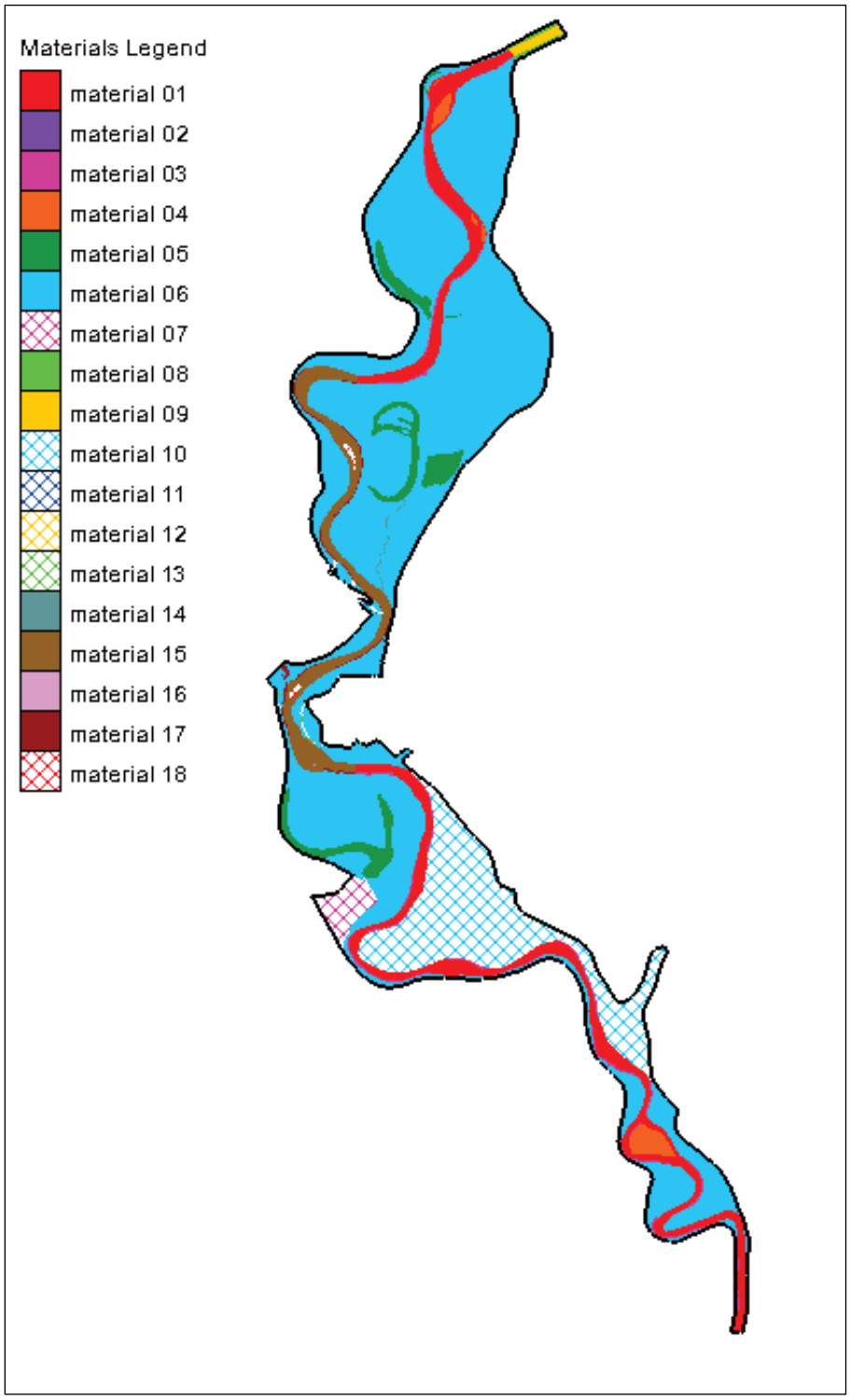

Table 15. Roughness parameters.

Material	Land Type	Manning's *n*	Unsubmerged Roughness, ft	Stem Diameter, ft	Density, ft^2
1	Channel	0.027			
2	Dikes	0.035			
3	Revetments	0.026			
4	Islands		0.16	3.28	0.11
5	Lakes	0.02			
6	Overbank		0.16	3.28	0.11
7	Forebay	0.02			
8	Morganza Reach		0.16	3.28	0.11
9	Artificial Natchez Reach	0.026			
10	Overbank Below Morganza		0.16	3.28	0.11
11	ORCC Channels	0.026			
12	ORCC Channels	0.026			
13	Angola Levees	0.026			
14	Buffalo River	0.027			
15	MS Channel Near ORCC	0.027			
16	Dikes near ORCC	0.035			
17	Revetments Near ORCC	0.026			
18	Islands Near ORCC		0.16	3.28	0.11

Table 16 lists the range of flows and headwaters that the physical model intended to simulate, and therefore the AdH model was simulated all the flow conditions presented in Table 16. The model boundaries included the inflow from the Mississippi River, the outflows from Hydropower, Low Sill Structure, and a stage at Baton Rouge. The flows through the Auxiliary and Overbank Structures were assumed to be zero. To obtain the tailwater at Baton Rouge, a rating curve was developed (Figure 24) by analyzing the flows and stages from the year 2000 to 2017. The rating curve relation developed is presented in Equation 6 below.

$$\eta = -0.0000174671Q^2 + 0.0587545821Q - 5.1349126774 \quad (6)$$

where, η is the stage in ft and Q is the flow at Baton Rouge in thousands of cubic feet per second.

Table 16. Flow and headwater scenarios simulated.

Δ H (ft)	Q MS Upstream (kcfs)	HW (ft)	Q Through Hydropower (kcfs)	Q Through Low Sill (kcfs)
35	1750	65.5	130	120
35	1130	55	130	50
30	1650	64	130	170
30	1100	54	130	70
25	1645	62.5	130	240
25	1015	52	130	85
20	1550	61	130	245
20	925	48	130	95
20	625	36.5	130	20
15	1480	60	130	300
15	775	40	130	70
15	640	35	130	60
10	1530	58	130	300
10	480	28	130	25

Figure 24. Rating curve for Baton Rouge.

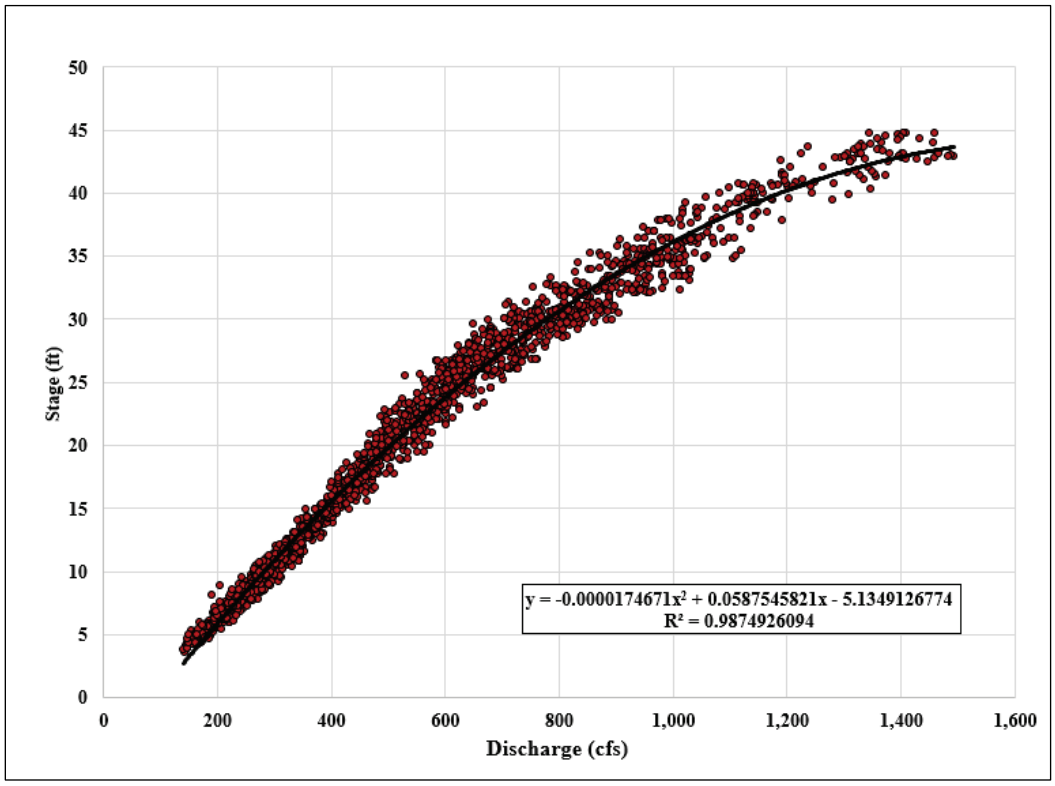

For each of the flow conditions presented in Table 16, the AdH model was executed for a period of 30 days or till steady state conditions were achieved. In all flow conditions, the model attained stated state in approximately 15 days. The model-simulated headwaters at the Low Sill structure were compared to those presented in Table 16. In all simulations, the AdH model accurately captured the head water reported in the field, with the greatest error of 2.4 ft or 3.96% occurring for a flow of 1550 kcfs. The results of these comparisons are presented in Figure 25.

Figure 25. Numerical vs. observed headwaters at LSCS.

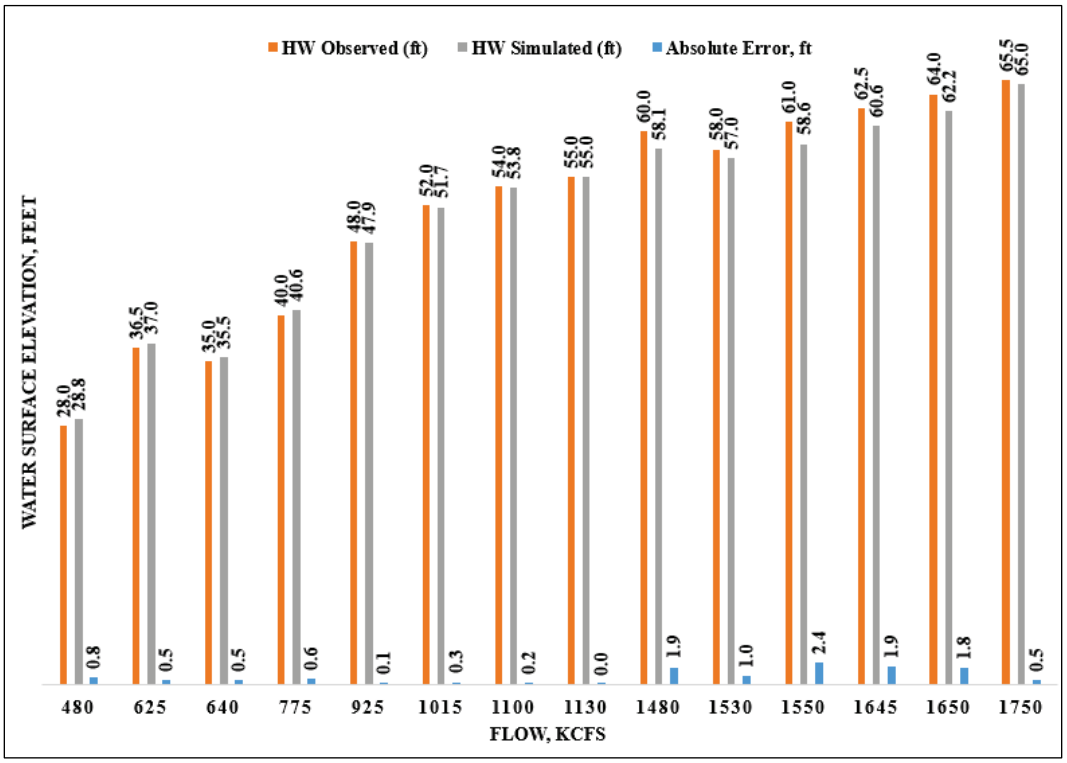

At the completion of the simulations, the velocity (directions and magnitudes) was analyzed at the upstream limits of the physical model (Figure 21). At this time, it was observed that the flow into the Low Sill structure channel was not perpendicular to the structure (an example from 625 kcfs simulation is provided in Figure 25) and that the physical model will require flow splits and directions to be provided from the numerical model. Figure 26 also illustrates the flow split locations provided to the physical model from the numerical model. The length of splits 1, 2, and 8 varied dependent upon any recirculating flow observed.

Figure 26. Example of flow to the LSCS.

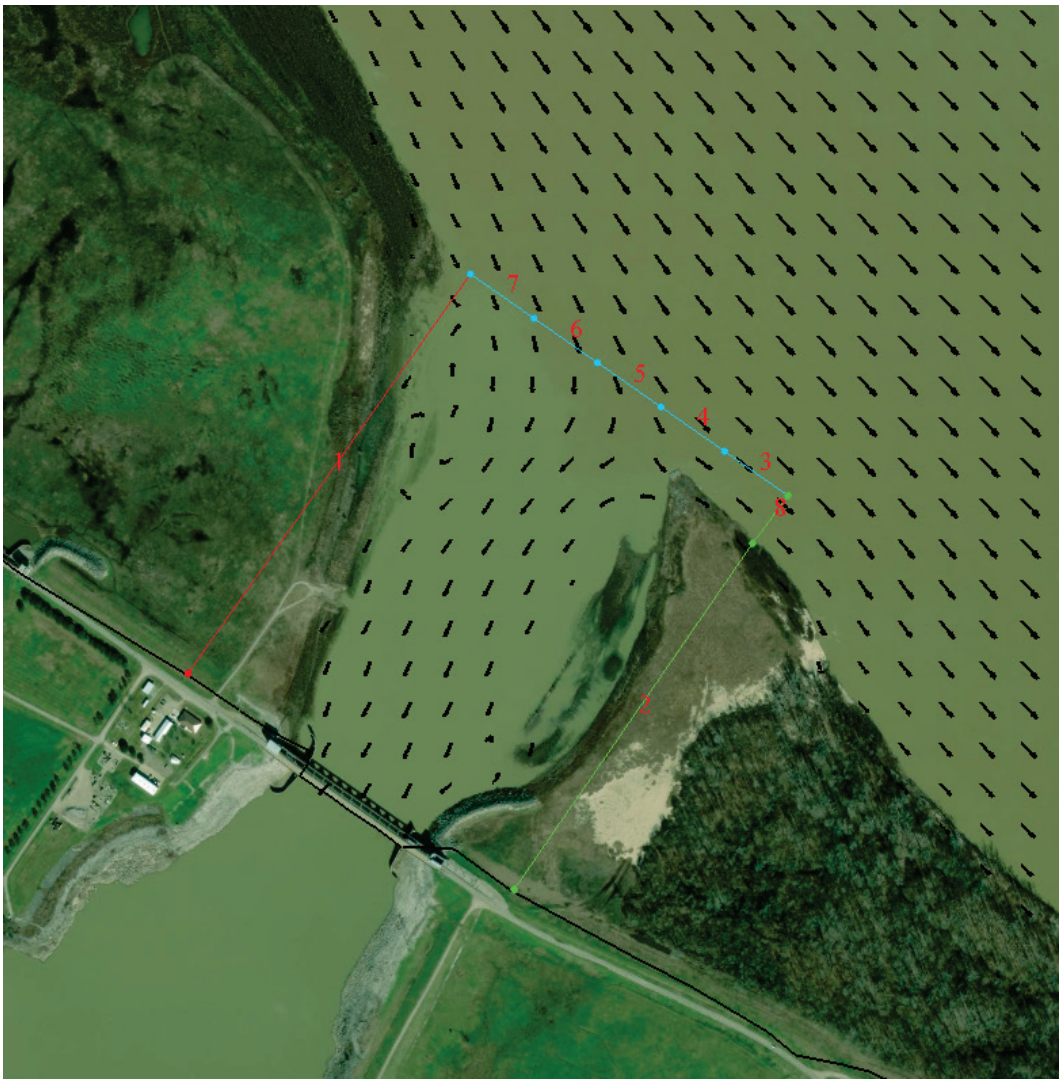

Unit Conversion Factors

Multiply	By	To Obtain
feet	0.3048	meters
inches	0.0254	meters
miles (US statute)	1,609.347	meters

Acronyms and Abbreviations

3D	Three-dimensional
AdH	Adaptive Hydraulics
CHL	Coastal and Hydraulics Laboratory
ERDC	US Army Engineer Research and Development Center
ID	Identifier
LSCS	Low-Sill Control Structure
MVN	New Orleans District
NAVD 88	North American Vertical Datum 1988
ORCC	Old River Control Complex
SI	International System of Units
USACE	US Army Corps of Engineers
WES	Waterways Experiment Station
WSE	Water surface elevation

REPORT DOCUMENTATION PAGE

Form Approved
OMB No. 0704-0188

1. REPORT DATE	2. REPORT TYPE	3. DATES COVERED *(From - To)*
May 2022	Final Report	FY19–FY20

4. TITLE AND SUBTITLE
Low-Sill Control Structure Gate Load Study

5a. CONTRACT NUMBER

5b. GRANT NUMBER

5c. PROGRAM ELEMENT NUMBER

6. AUTHOR(S)
Jeremy A. Sharp, Duncan B. Bryant, and Gaurav Savant

5d. PROJECT NUMBER

5e. TASK NUMBER

5f. WORK UNIT NUMBER

7. PERFORMING ORGANIZATION NAME(S) AND ADDRESS(ES)
Coastal and Hydraulics Laboratory
US Army Engineer Research and Development Center
3909 Halls Ferry Road
Vicksburg, MS 39180-6199

8. PERFORMING ORGANIZATION REPORT NUMBER
ERDC/CHL TR-22-8

9. SPONSORING/MONITORING AGENCY NAME(S) AND ADDRESS(ES)
US Army Corps of Engineers, New Orleans District
New Orleans, LA 70118

10. SPONSOR/MONITOR'S ACRONYM(S)
USACE MVN

11. SPONSOR/MONITOR'S REPORT NUMBER(S)

12. DISTRIBUTION/AVAILABILITY STATEMENT
Approved for public release; distribution is unlimited.

13. SUPPLEMENTARY NOTES
MIPRs W42HEM00279380, W42HEM00772956

14. ABSTRACT

The effort performed here describes the process to determine the gate lifting loads at the Low-Sill Control Structure. To measure the gate loads, a 1:55 Froude-scaled model of the Low-Sill Control Structure was tested. Load cells were placed on 3 of the 11 gates. Tests evaluated the gate loads for various hydraulic heads across the structure. A total of 109 tests were conducted for 14 flows with each flow having two gate settings provided by the United States Army Corps of Engineers, New Orleans District. The load data illustrated the potential for higher gate lifting loads (GLL) to occur at the mid-range gate opening (Go) for Gates 3 and 6. While for Gate 10, the highest GLL (452 kips, maximum load in testing) was at a Go = 4.2 ft. Conversely, for the low-flow bays, the highest load occurred at Go = 24.86 ft.

15. SUBJECT TERMS
Concordia Parish (La.), Diversion structures (Hydraulic engineering), Hydraulic gates, Hydraulic models, Mississippi River

16. SECURITY CLASSIFICATION OF:			17. LIMITATION OF ABSTRACT	18. NUMBER OF PAGES	19a. NAME OF RESPONSIBLE PERSON
a. REPORT	b. ABSTRACT	c. THIS PAGE			Jeremy A. Sharp
Unclassified	Unclassified	Unclassified	SAR	63	19b. TELEPHONE NUMBER *(Include area code)* 601-634-4212